

REVIEW

Open Access



# Recent progress of quantum dots for energy storage applications

Quan Xu<sup>1</sup>, Yingchun Niu<sup>1</sup>, Jiapeng Li<sup>1</sup>, Ziji Yang<sup>1</sup>, Jiajia Gao<sup>1</sup>, Lan Ding<sup>1</sup>, Huiqin Ni<sup>1</sup>, Peide Zhu<sup>1</sup>, Yinping Liu<sup>1</sup>, Yaoyao Tang<sup>1</sup>, Zhong-Peng Lv<sup>2</sup>, Bo Peng<sup>2</sup>, Travis Shihao Hu<sup>3</sup>, Hongjun Zhou<sup>1</sup> and Chunming Xu<sup>1\*</sup>

## Abstract

The environmental problems of global warming and fossil fuel depletion are increasingly severe, and the demand for energy conversion and storage is increasing. Ecological issues such as global warming and fossil fuel depletion are increasingly stringent, increasing energy conversion and storage needs. The rapid development of clean energy, such as solar energy, wind energy and hydrogen energy, is expected to be the key to solve the energy problem. Several excellent literature works have highlighted quantum dots in supercapacitors, lithium-sulfur batteries, and photocatalytic hydrogen production. Here, we outline the latest achievements of quantum dots and their composites materials in those energy storage applications. Moreover, we rationally analyze the shortcomings of quantum dots in energy storage and conversion, and predict the future development trend, challenges, and opportunities of quantum dots research.

**Keywords:** Quantum Dots, electrochemical, photocatalytic, energy storage

## 1 Introduction

Decarbonized clean energy such as solar energy, wind energy and geothermal energy has become the solution to global warming, energy crisis and environmental pollution [1]. In the context of carbon neutrality, new energy will become the main source of electricity, and the storage of large amounts of renewable energy will be a major challenge [2]. However, these energy sources are intermittent in nature, so they need to be stored and released at any time [3, 4]. Electrochemical energy storage such as batteries [5, 6] and supercapacitors [7, 8] will become the main idea to deal with this dilemma. In addition, photocatalytic hydrogen evolution is based on supporting electrochemical hydride formation and photochemical bonding to form fuel, which is also a "clean" method of energy storage [9, 10].

In recent years, quantum dots have attracted extensive attention for their potential electrochemical energy

storage due to their large specific surface area, adjustable size, short ion/electron transport path, non-toxicity, low cost, adjustable photoluminescence, and easy surface functionalization [11–13]. Global warming and the consumption of fossil fuels have caused increasing environmental problems. Quantum dots (QDs) are rapidly developing in the field of energy storage and conversion. QDs are mainly spherical or quasi-spherical 0 nm materials with sizes less than 10 nm [14, 15]. Manufacturing methods are usually classified as "top-down" [16–18] and "bottom-up" [19–21]. In general, the top-down method usually takes massive materials as the precursor and obtains QDs through chemical etching, [22–24] microwave irradiation, [25–27] ultrasonic treatment, [28–30] electrochemical method, [3, 4, 31] hydrothermal/solvothermal method [32–34] and other methods [35–37]. QDs can also be chemically assembled from small organic and inorganic precursors by a bottom-up synthesis strategy [38–40]. QDs have been synthesized in various ways to be zero-dimension materials, which show unusual chemical and physical properties due to their strong quantum confinement and edge effect, and obtain high bandgap, ultra-small size, and high

\* Correspondence: [xuquan@cup.edu.cn](mailto:xuquan@cup.edu.cn)

<sup>1</sup>State Key Laboratory of Heavy Oil Processing, China University of Petroleum-Beijing, Beijing 102249, China  
Full list of author information is available at the end of the article

surface-area-to-volume ratio [11, 41]. The size, structure, functional groups, and heteroatomic parameters can also be regulated during the synthesis of QDs. As such, their active sites per unit mass, physicochemical tunability, and adaptability to hybridization with other nanomaterials are improved [42, 43].

The overall performance of an electrochemical energy storage system is highly dependent on the electrode materials used [44–46]. The heteroatomic functional groups are rich in the surface of QDs, providing a wide range of active sites. They can be used as composite materials for current collector [47, 48] and active electrode [49, 50], showing superior ionic conductivity, [51] high rate, [52] large capacity, [53] and cycle stability, [54] significantly improving the performance of electrochemical energy storage devices. Chakrabarty et al. reported a  $\text{CeO}_2/\text{Ce}_2\text{O}_3$  quantum dot to enhance the electrocatalytic activity of reduced graphene oxide (RGO) electrodes in supercapacitors [55]. Carbonaceous materials are the most promising candidates for the anode of sodium-ion batteries [56]. Liu et al. constructed CQD modified  $\text{Na}_3\text{V}_2(\text{PO}_4)_2\text{F}_3$  graded microspheres. The cathode of sodium-ion battery with ultra-high capacity and satisfactory rate performance [57]. Sun et al. used rGO riveted bismuth oxychloride as a high-performance anode for SIB by inducing the interface BI-C bond. Compared with other metal halogen oxide anodes, the charging capacity and cycling stability of SIB prepared by using it have been greatly improved [58]. The synergy between the crystal field and the stability energy of the coordination field of OH coordination Fe in ferric hexadecyanite can induce the embedded pseudo capacitance [59]. The unique electron donor and acceptor properties and excellent electron transfer properties make QD a highly efficient and stable photocatalyst for hydrogen evolution, oxygen reduction, and oxygen evolution reactions [60–63]. Photocatalysis integrates photocatalysis and electrocatalysis. Photocatalytic hydrogen production is an important prerequisite of photocatalytic hydrogen production [64]. Recent studies on QDs have also demonstrated their great potential in the field of photocatalysis [65–67]. Elsayed et al. prepared heterogeneous photocatalysts in the form of polymer dots by combining organic semiconductor polymers with N-doped carbon quantum dots covered by PS-PEGCOOH, and its hydrogen evolution rate increased by about five times [68]. In addition, heteroatoms doped on QDs can form strong interactions with hydrogen, increasing adsorption capacity, which is also promising for hydrogen storage [69, 70].

In this review, the latest progress in the field of QDs is comprehensively summarized, including the preparation and mechanism of QD composites in electrochemical

and photocatalytic systems, energy storage (electrochemical capacitors, lithium/sulfur batteries), and photocatalysis (hydrogen evolution). Finally, we discuss the advantages and disadvantages of QDs in electric energy storage and photocatalytic hydrogen evolution, make a prospect of QDs for hydrogen storage, and suggest the remaining challenges and opportunities.

## 2 Application of quantum dots in lithium- sulfur batteries

Sulfur cathode materials in rechargeable lithium-sulfur (Li-S) batteries have a high theoretical capacity and specific energy density, low cost, and meet the requirements of portable high electric storage devices [71]. Due to their small particle size, large surface area, and adjustable surface function, [72] quantum dots (QDs) can be used as the modified material of positive electrodes [73, 74] and separator [75] materials in Li-S batteries. Ions in batteries can obtain a short transmission path and a fast conduction rate [76–78].

### 2.1 Positive electrode for lithium-sulfur batteries

The theoretical capacity of sulfur cathode materials in Li-S batteries is up to  $1675 \text{ mAh g}^{-1}$ . Unlike traditional cathode insertion materials, sulfur undergoes a series of composition and structure changes during the cycle, forming soluble polysulfides and insoluble sulfides. Therefore, the practical application of Li-S batteries has been plagued by several fundamental challenges, [79–81] such as the low conductivity of sulfur and its discharge products ( $\text{Li}_2\text{S}_2/\text{Li}_2\text{S}$ ), the shuttle of intermediate polysulfides during the recharge/discharge process, and the significant volume expansion of sulfur. Quantum dots have a high specific surface area and many surface functional sites, which provide abundant active sites for the absorption and localization of polysulfides. It can achieve a high sulfur load to reduce polysulfide shuttle and accommodate the volume expansion of sulfur particles.

In this context, we summarize various quantum dots that capture polysulfides near the cathode. Gao et al. reported for the first time a simple, one-step strategy for growing  $\text{TiO}_2$  quantum dots on ultra-thin MXene ( $\text{Ti}_3\text{C}_2\text{T}_x$ ) nanosheets *via* solvothermal synthesis assisted by cetyltrimethylammonium bromide (CTAB) [82]. Due to the presence of CTAB, this strategy can well protect MXene from oxidation, so the obtained  $\text{TiO}_2\text{QDs@MXene}$  nanohybrid has high conductivity to ensure rapid ion diffusion and inhibits the shuttle effect of polysulfide. Because of its ultra-thin properties, the nanohybrid retains most of the active region characteristics to adapt to the volume expansion of loaded sulfur particles. As shown in Fig. 1A, the shuttle effect of polysulfide can also be inhibited.  $\text{TiO}_2$  QDs@MXene/S negative electrodes provide capacities up to 1158, 1037, 925, 812, and

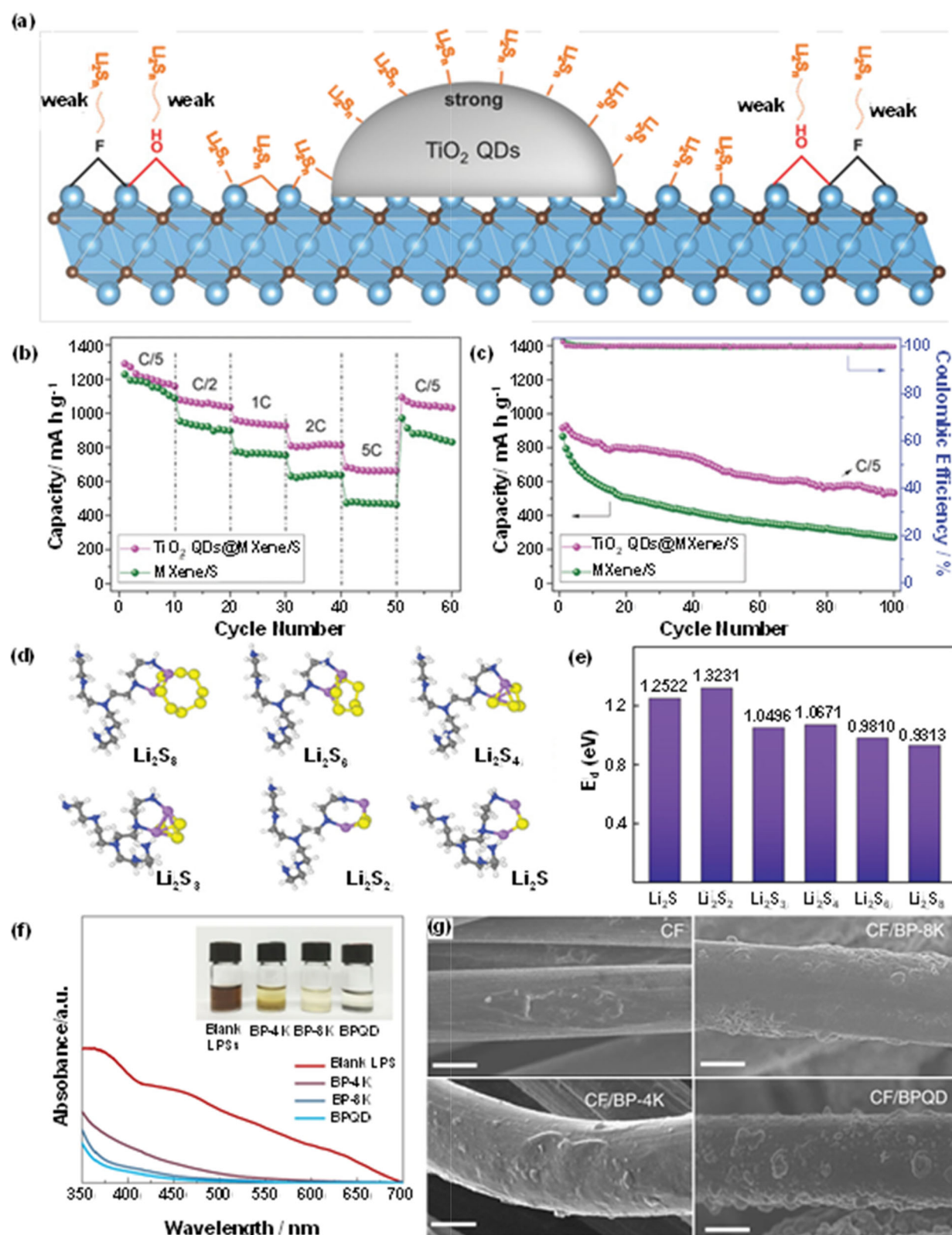


Fig. 1 (See legend on next page.)

(See figure on previous page.)

**Fig. 1** **A** Schematic diagram of the principle of TiO<sub>2</sub> quantum dots growing on MXene nanosheets to inhibit the polysulfide shuttle effect; **B** rate capabilities of TiO<sub>2</sub> QDs/MXene/S and MXene/S cathodes (1C = 1675 mA g<sup>-1</sup>); **C** Comparisons of cycle behaviors at C/5 (sulfur loading = 5.5 mg cm<sup>-2</sup>) of TiO<sub>2</sub> QDs/MXene/S and MXene/S cathodes; (Reprinted from Ref. [82]. Copyright 2018 Wiley-VCH.) **D** The calculated configurations of the LiPSs species (Li<sub>2</sub>S, Li<sub>2</sub>S<sub>2</sub>, Li<sub>2</sub>S<sub>3</sub>, Li<sub>2</sub>S<sub>4</sub>, Li<sub>2</sub>S<sub>6</sub>, and Li<sub>2</sub>S<sub>8</sub>) on a reducible molecular structure of the PEI surface functional groups; **E** The calculated binding energy between the PEI surface-active group and the LiPSs species; (Reprinted from Ref. [83]. Copyright 2019 Wiley-VCH.) **F** SEM images of Li<sub>2</sub>S precipitation on different substrates; **G** UV-vis spectra of LiPS with variation in color upon adsorption by different-sized BP flakes. (CF is carbon fiber, BP-4K is BP that was centrifuged at 4000 rpm, BP-8K was centrifuged at 8000 rpm, BPQD is black phosphorus quantum dot) (Reprinted from Ref. [81]. Copyright 2018 SPRINGER NATURE.)

663 mAh g<sup>-1</sup> when cycled at C/5, C/2, 1C, 2C, and 5C rates (1C = 1675 mA g<sup>-1</sup>). In contrast, the capacities of MXene/S cathodes at the same rate are only 1088, 897, 753, 636, and 464 mAh g<sup>-1</sup> (Fig. 1B and C). Hu et al. designed and prepared polyethyleneimine functionalized carbon dots (PEI-Cdots) to improve the performance of Li-S batteries with high sulfur loads, suitable for operation under high current density conditions [83]. As shown in Fig. 1D and E, they also calculated the configuration of LiPSs functional groups on the PEI surface and the binding energy between them. The chemical binding and rapid ion transport properties of polysulfides were enhanced in the cathode modified by PEI-Cdots. It is noteworthy that black phosphorus has good volume conductivity, rapid lithium-ion diffusion constant [84], and high binding energy with sulfur, [85] which indicate that black phosphorus can be used as a carrier of polysulfides. Based on their adsorption and electrocatalysis studies, Xu et al. demonstrated that using nano-scale black phosphorus (BP) particles (such as BP quantum dots (BPQD)) could greatly improve the adsorption of polysulfides in black phosphorus [81]. They performed a LiPSs static adsorption experiment on a BP sheet, and the result was BPQD > BP-8K > BP-4K (Fig. 1F), consistent with UV-VIS spectra. Scanning electron microscope (SEM) images also showed that the precipitation effect of Li<sub>2</sub>S on CF/VPQD was the best. (Fig. 1G) They combined a small amount of BPQD (2% by weight of the positive electrode) with a sulfur/porous carbon fiber positive electrode. The Li-S battery did not show polysulfide diffusion while maintaining excellent battery performance.

## 2.2 Quantum dot modified separator

In the discharge/charging process of Li-S batteries, soluble polysulfide will diffuse into the liquid electrolyte and shuttle to the lithium negative electrode through the separator. It results in the passivation of the lithium negative electrode and the loss of active materials, leading to low coulomb efficiency and rapid capacity decay [86, 87]. Conventional separators cannot prevent the diffusion of soluble polysulfides [75]. Quantum dots can also modify the separator to reduce the shuttle effect of polysulfides due to their strong interaction with

polysulfides. We summarize the quantum dots used to assist in separator modification. Ding et al. used atomic layer deposition (ALD) to create a TiO<sub>2</sub> quantum dot-modified multi-walled carbon nanotube as a polypropylene separator for Li-S batteries [75]. This strategy can prevent soluble polysulfide from shuttling through the separator to the lithium anode and improve the coulomb efficiency and cycle stability of Li-S batteries. (Figure 2A) The Li-S battery with MWCNTs@TiO<sub>2</sub> quantum dots modified separator provides an initial capacity of 1083 mAh g<sup>-1</sup> and maintains a cycle capacity of 610 mAh g<sup>-1</sup> after 600 cycles at a rate of 838 mA g<sup>-1</sup>. It maintains an average capacity attenuation of only 0.072% per cycle. (Figure 2B) Pang et al. designed an ultralight coated diaphragm by coating one side of a commercial PP partition with ultralight multi-walled carbon nanotubes/N-doped carbon quantum dots (MWCNTs/NCQDs) [88] (Fig. 2C). The area weight of MWCNTs/NCQDs coating was as low as 0.15 mg cm<sup>-2</sup> (Fig. 2D). Compared with the MWCNTs modified diaphragm designed by Chung et al. [90] the capacity retention and self-discharge inhibition of Li-S batteries using MWCNTs/NCQDs layer separator was improved. The synergistic effect of MWCNTs and NCQDs resulted in a relatively high initial discharge capacity of 1330.8 mAh g<sup>-1</sup> and excellent cycling performance. The corresponding capacity attenuation rate was as low as 0.05% per cycle at 0.5 C, exceeding 1000 cycles (Fig. 2E). It is worth noting that the lithium metal anode in the lithium-ion battery will lead to the uncontrolled growth of lithium dendrites during the continuous charging and discharging process, which may lead to low coulomb efficiency and safety problems [91, 92]. To address these problems, Yu et al. designed a novel Mo<sub>2</sub>C quantum dot (MQD) anchored N-doped graphene (NG) functionalized separator (MQD@NG) [89]. As shown in Fig. 2F, the optical and TEM images of MQD@NG/PP separator after 200 cycles show that the lithophile of polar Mo<sub>2</sub>C QDS can establish a fast electrolyte diffusion path for lithium ions, achieving uniform deposition of lithium and having strong chemical adsorption of polysulfide. The Li-S battery with an MQD@NG interlayer achieved more than 1600 hours of dendrite-free lithium deposition at a high current density of 10 mA cm<sup>-2</sup>. The battery also has a



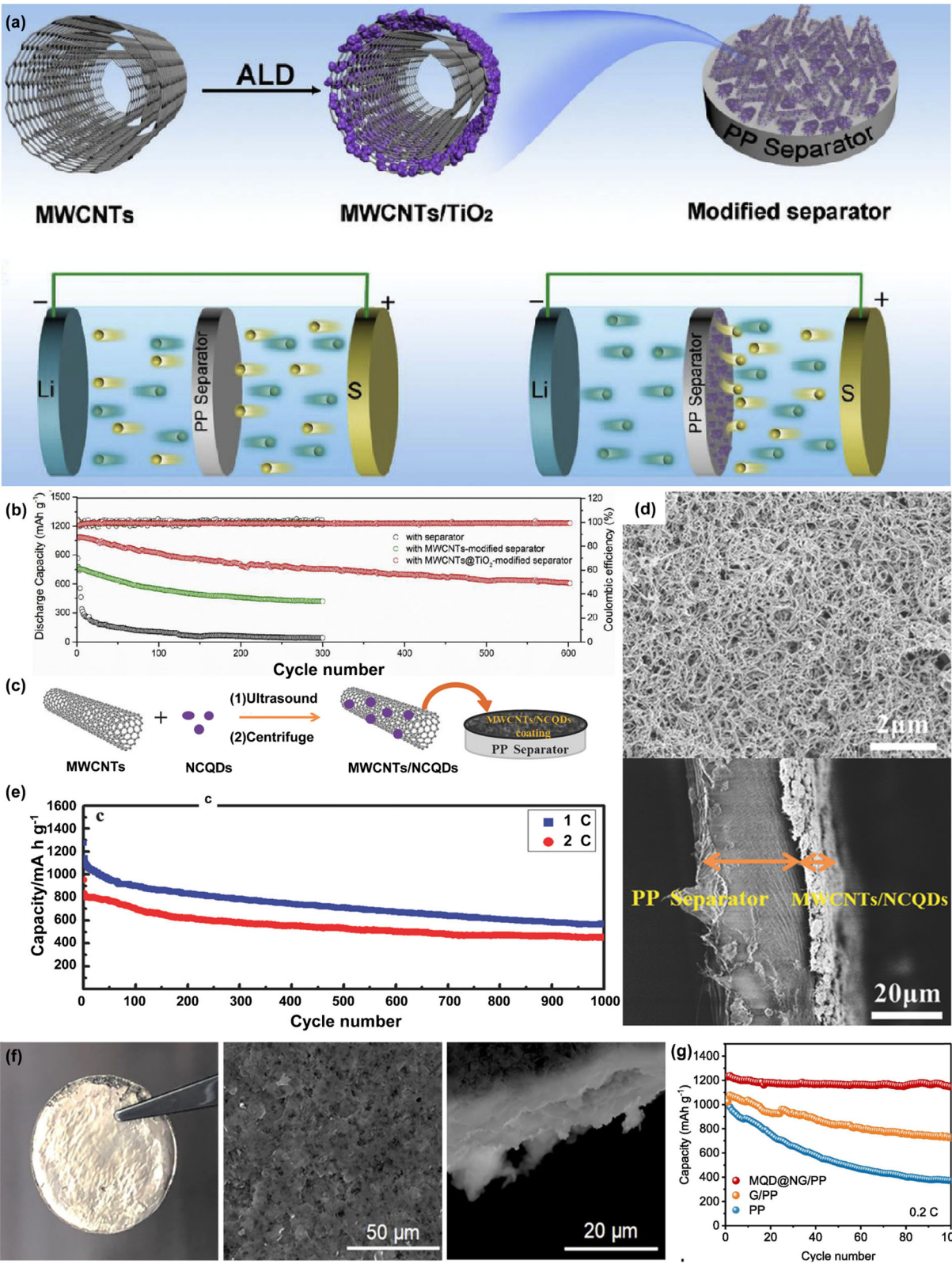


Fig. 2 (See legend on next page.)

(See figure on previous page.)

**Fig. 2 A** schematic diagram of the preparation process of MWCNTs@TiO<sub>2</sub> quantum dots and Schematic diagram of li-S cell with commercial PP diaphragm and MWCNTs@TiO<sub>2</sub> quantum dot coated diaphragm; **B** Long life cycle tests of Celgard, MWCNTs/Celgard and MWCNTs@TiO<sub>2</sub> quantum dots /Celgard. (Reprinted from Ref. [75]. Copyright 2018 Elsevier Ltd.) **C** Schematic diagram of BPQD/TNS composite and HRTEM image of BPQD anchored on TNS surface; **D** Photographs of one side of the MWCNTs/NCQDs-coated separator and cross-section of MWCNTs/NCQDs-coated separator; **E** Long-term cycling performance at 1 and 2 C of the Li-S batteries with MWCNTs/NCQDs-coated separator.(Reprinted from Ref. [88]. Copyright 2018 Wiley-VCH.) **F** Optical photograph of the lithium plate after plating/stripping with MQD@NG/PP separators for 200 cycles. Corresponding SEM image of the lithium plate with MQD@NG/PP separator. cross-section of the lithium plate after cycles. **G** Cycle performance of PP, G@PP, MQD@NG/PP batteries at 0.2c. (Reprinted from Ref. [89]. Copyright 2020 Elsevier Ltd.)

high capacity of 1230 mAh g<sup>-1</sup> with highly stable cycle performance after 0.2C and 100 cycles without significant capacity attenuation. Figure 2G

In this section, we discuss the application progress of quantum dots in li-S cathode and diaphragm components. By introducing quantum dots into the positive electrode and diaphragm of lithium-sulfur battery, the surface properties and adjustable ligands of quantum dots are utilized to improve the adsorption of soluble polysulfide and inhibit "shuttle effect", and the charge capacity and cyclic stability of the battery are improved remarkably. At present, there are some new ways to solve the crossing effect of polysulfide. For example, Ye et al use different catalysts to degrade polysulfide at  $S_8 \leftrightarrow Li_2S_4$  and  $Li_2S_4 \leftrightarrow Li_2S$  [93]. This may provide a new idea for the application of quantum dots in Li-S batteries. It is believed that more and more quantum dots will be introduced into the preparation of cathode, diaphragm, and even positive electrode and electrolyte of Li-S batteries. Here, we propose some problems that need to be solved for the preparation of relevant quantum dots in the future and possible research trends in the future. Firstly, the structure and chemical properties of the designed quantum dots should be correlated with the electrochemical performance of Li-S cells, so that they can play their excellent inherent properties in the battery environment. Secondly, the mechanical properties of quantum dot composites and the adsorption of polysulfide can maintain long-term stability in the use and preparation. Finally, if li-S batteries are to be used in large numbers in real life, it is necessary to optimize or design a new preparation process to minimize the preparation cost of quantum dot composites.

### 3 Progress of quantum dots in supercapacitors

Supercapacitors (SCs) have been widely concerned by researchers in recent years due to their higher power density, long cycle life, and fast charge and discharge [94–96]. Fig. 3A shows the structure of traditional capacitors and supercapacitors, SCs are composed of electrodes immersed in the electrolyte, and a diaphragm electrically isolates the electrodes. According to different energy storage mechanisms, SCs can be divided into two types: double-layer capacitors (DLCs)

represented by adsorption-desorption energy storage, and the other is pseudocapacitors materials represented by hydrogen storage by a redox reaction [48, 101]. Compared with traditional batteries, the lower energy density of SCs limits the development of their practical applications. Thus, researchers have done a lot of research to improve the energy density of SCs and develop new electrode materials with strong cycle stability and high capacity. CDs-based electrodes can provide ultra-high capacity and maximum efficiency due to their excellent properties, such as excellent electronic conductivity, lots of active sites, high surface area, significant wettability in different solvents, and adjustable bandgap. Carbon /graphene quantum dots (CQDs or GQDs) retain the characteristics of carbon materials' stable chemical properties and have quantum tunneling effect, size effect, and surface effect. It has a strong adsorption capacity for electrolyte ions, and it has a wide range of development prospects in SCs [95, 98, 101, 102]. Table 1 summarizes carbon-based quantum dots in enhancing supercapacitors in recent years. Studies have shown that the energy density of SCs based on GQDs is closer to that of batteries [95, 112].

The DLCs is mainly based on charge storage, and the electrode material is mainly carbon material of high ratio surface area [113]. The application of quantum dots in double-layer capacitors is to embed quantum dots in carbon electrode materials to increase the specific surface area of carbon materials, so as to obtain higher SC performance. For example, Qing et al. [97] embedded highly crystalline GQDs into activated carbon and constructed a conductive network as shown in Fig. 3B, which promoted the storage of electrolyte ions in deep pores and improved the electrochemical performance of activated carbon. Generally speaking, GQDs can shorten the ion transmission path due to their nano-size constructability and highly crystalline conductive properties. As an emerging material for DLCs electrodes, carbon nanofibers have strong mechanical properties, large specific surface area and good electrical conductivity (Fig. 3C) [114]. However, it is challenging to have both porous structure and conductive network to ensure the structural stability and good conductivity of carbon nanofibers electrodes. Zhang et al. [99] found that

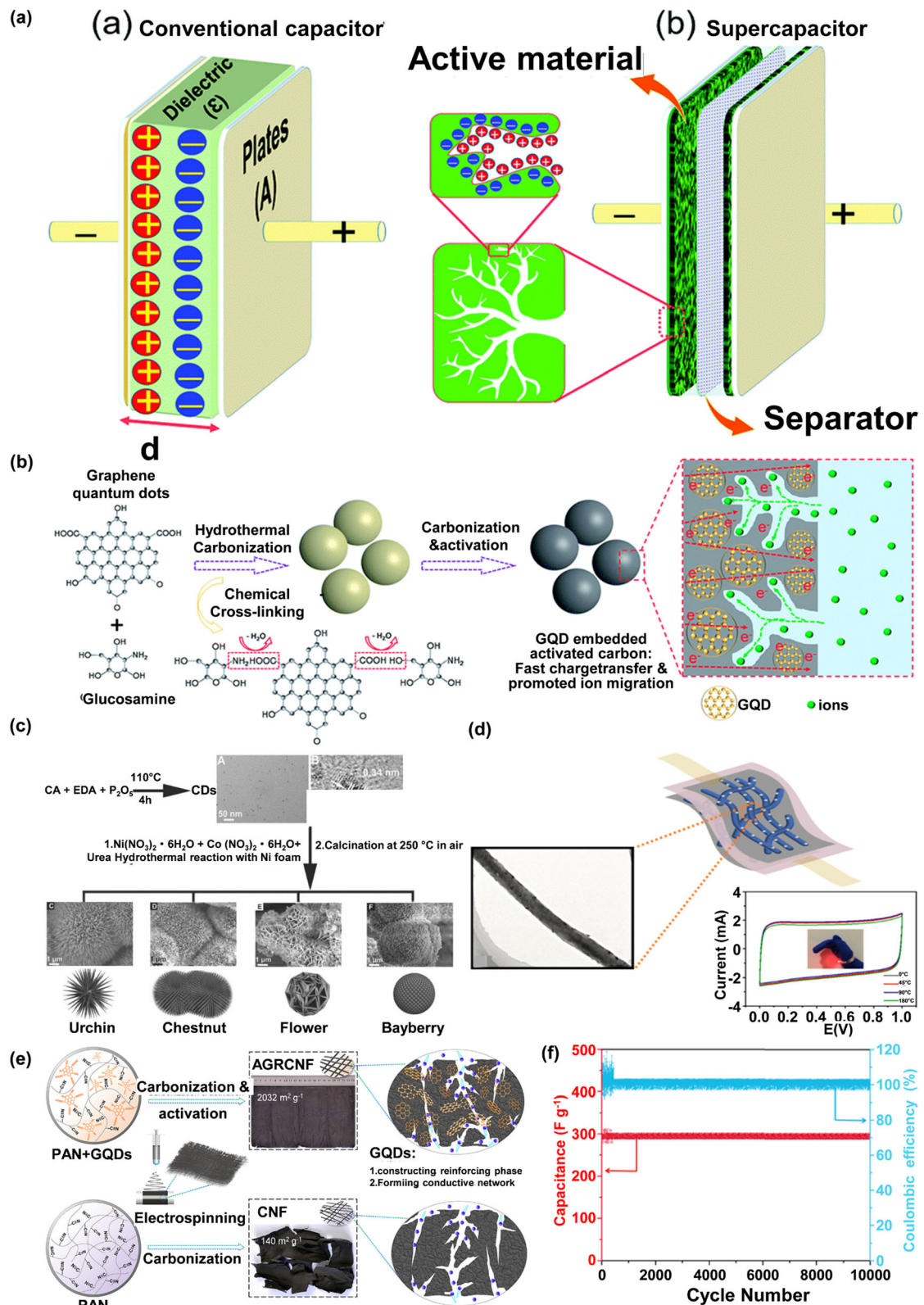


Fig. 3 (See legend on next page.)



(See figure on previous page.)

**Fig. 3 A** Schematic representation of a conventional capacitor and a supercapacitor; (Reprinted from Ref. [96]. Copyright 2019 Royal Society of Chemistry.) **B** Illustration of the N-GQDs//MoS<sub>2</sub>-QDs asymmetric MSCs; (Reprinted from Ref. [97]. Copyright 2019 Royal Society of Chemistry.) **C** The CDs are synthesized hydrothermally with uniform sizes and employed to prepare C–F the CDs/NiCo<sub>2</sub>O<sub>4</sub> composites with different morphologies; (Reprinted from Ref. [98]. Copyright 2016 Wiley-VCH.) **D** Schematic diagram of graphene quantum dots modified carbon nanofiber felt flexible supercapacitor; (Reprinted from Ref. [99]. Copyright 2021 Royal Society of Chemistry.) **E** Schematic diagram of GQD-reinforced electrospun carbon nanofiber fabrics (AGRCNF) prepared by electrostatic spinning, carbonization and chemical activation; **F** Cycle performance of the AGRCNF-3//AGRCNF-3 supercapacitor at 50 A g<sup>-1</sup>. (Reprinted from Ref. [100]. Copyright 2020 ACS Publications)

carbon nanofiber mats modified with GQDs can significantly improve the mechanical and electrochemical performance of flexible supercapacitors (Fig. 3D). The content of quantum dots can adjust the degree of cross-linking between carbon nanofibers. The cross-linked fiber structure can improve the mechanical and electrical properties of the carbon nanofiber mat. Zhao et al. [100] integrated GQDs into electrospun carbon fiber (Fig. 3E), which play an essential role in constructing reinforcing phase and conductivity. What's more, the device can charge the capacitor to 80% in only 2.2s, and the capacity does not decay significantly after 10,000 cycles at 50 Ag<sup>-1</sup> (Fig. 3F). That shows a vast development prospect as a back up power source power source.

Pseudocapacitance is associated with the electrical adsorption and surface REDOX processes of large areas of electrode materials, usually metal oxides and conductive polymers [113]. QDs can be combined with other materials such as conductive polymers, transition metal oxides, etc., as electrodes materials. Combining CDs and GQDs in metal oxides can improve their conductivity and conductivity performance. Wei et al. [114] used the hydrothermal method and calcination treatment to combine CDs/NiCo<sub>2</sub>O<sub>4</sub> as the electrode material of SCs, the addition of CDs accelerates the diffusion between electrodes and ions. Jia et al. [94] prepared the GQDs/MnO<sub>2</sub> heterostructure electrode by a simple two-step method (hydrothermal and plasma vapor deposition method). The prepared GQDs with a particle size of 2–3 nm are

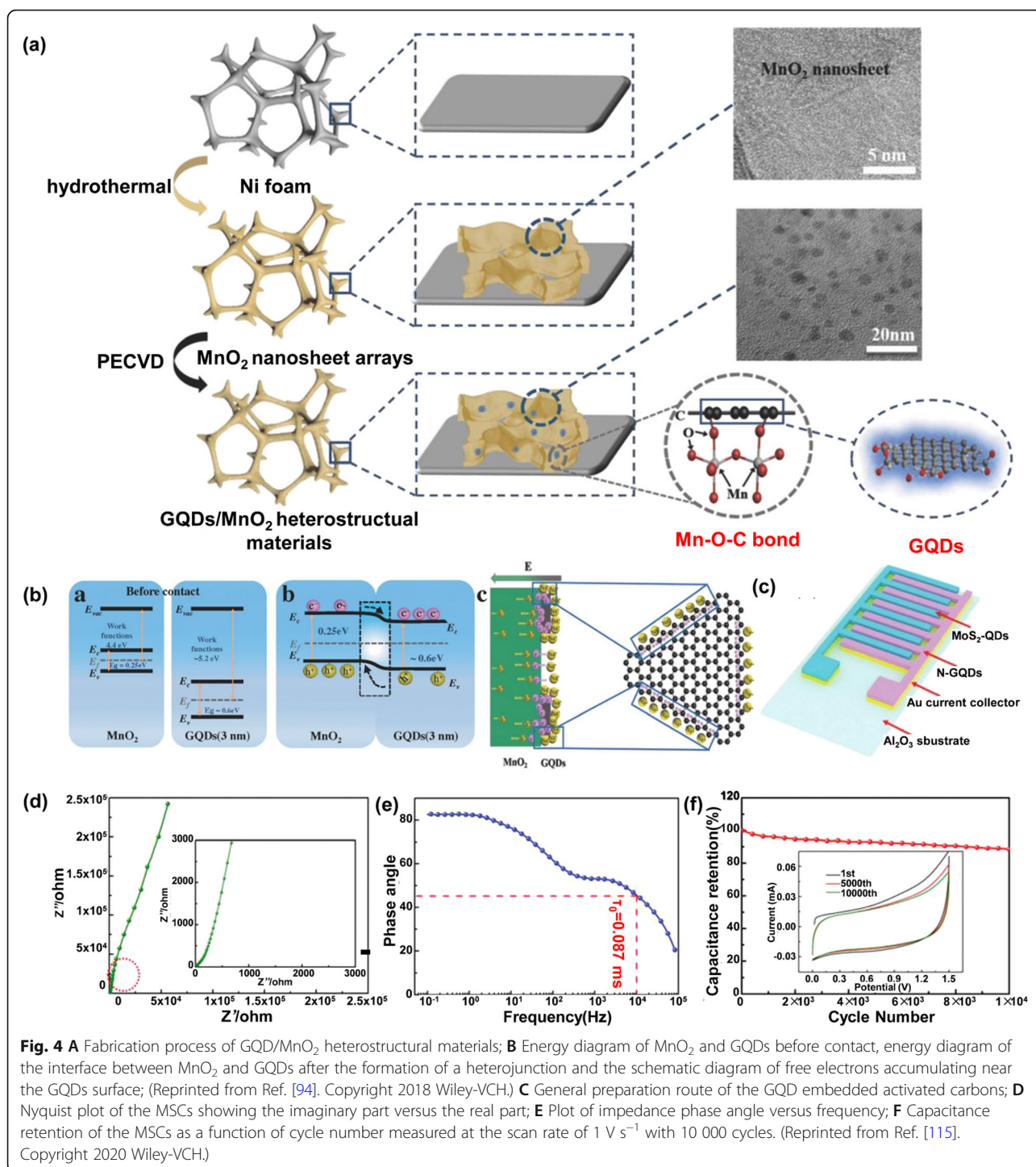
dispersed on the surface of MnO<sub>2</sub>, and the GQDs/MnO<sub>2</sub> composite material is prepared by controlling the deposition time (Fig. 4A). The potential window of the high-performance water SC reaches 1.3V. The schematic diagram of energy change before and after contact with MnO<sub>2</sub> and GQDs is shown in Fig. 4B. Because GQDs has a huge active site and high conductivity.

It is worth noting that in recent years, some studies have directly used quantum dots as electrodes, which have significant advantages as electrode materials for micro SCs (MSCs) [116, 117]. As shown in Fig. 4C, Liu et al. [115] used molybdenum disulfide quantum dots (MoS<sub>2</sub>-QDs) and nitrogen-doped GQDs (N-GQDs) as cathode and anode materials, respectively, and the prepared micro-supercapacitors (MSCs) showed excellent electrochemical performance. Through heteroatom doping, it produces abundant functional groups on the surface, forming structural defects and then adjusting the physical and chemical properties of the material. GQDs can be used not only as an electrode material for SCs but also as an electrolyte. The characterization of SCs by electrochemical impedance spectroscopy explains the reasons for their remarkable chemical properties. As shown in Fig. 4D, the Nyquist plot showed a nearly straight line along the imaginary axis, indicating that the resulting MSCs have near-capacitive behavior. The relaxation time constant of n-GQDs // MoS<sub>2</sub>-QDs asymmetric MSCs prepared by them was 0.087ms (Fig. 4E), which was much lower than most reported onion-like

**Table 1** Application of quantum dots in supercapacitors

Electrode materials	Specific capacitance	Cycling life	Electrolyte	Energy density	Ref
NiCo <sub>2</sub> O <sub>4</sub> /GQDs	481.4 F g <sup>-1</sup> at 0.35 Ag <sup>-1</sup>	65.88% (300)	1M KOH	-	[103]
GQDs	332 F g <sup>-1</sup> at 0.5 Ag <sup>-1</sup>	-	1M H <sub>2</sub> SO <sub>4</sub>	6.4 Wh kg <sup>-1</sup>	[99]
CQDs/Ni <sub>3</sub> S <sub>2</sub>	1130 F g <sup>-1</sup> at 2 Ag <sup>-1</sup>	80% (3000)	1M KOH	18.8 Wh kg <sup>-1</sup>	[104]
NCH/NCQDs	727 C g <sup>-1</sup> at 1 A g <sup>-1</sup>	87.5% (8000)	3M KOH	49.1 Wh kg <sup>-1</sup>	[105]
NiCo <sub>2</sub> O <sub>4</sub> /CQDs	856 F g <sup>-1</sup> at 1A g <sup>-1</sup>	98.75% (10000)	2M KOH	13.1 Wh kg <sup>-1</sup>	[106]
V <sub>2</sub> O <sub>5</sub> /GQDs	572 F g <sup>-1</sup> at 1A g <sup>-1</sup>	92% (10000)	0.1 M H <sub>2</sub> SO <sub>4</sub>	31.25 Wh kg <sup>-1</sup>	[107]
ONCDs/Porous Hydrogels	400 F g <sup>-1</sup> at 1A g <sup>-1</sup>	100% (10000)	1M H <sub>2</sub> SO <sub>4</sub>	13.5 Wh kg <sup>-1</sup>	[108]
MnO <sub>2</sub> /CQDs	340 F g <sup>-1</sup> at 1A g <sup>-1</sup>	80.1% (10000)	1M Na <sub>2</sub> SO <sub>4</sub>	33.6 Wh kg <sup>-1</sup>	[109]
GQDs/Ultra microporous	3 F cm <sup>-2</sup> at 0.5 A g <sup>-1</sup>	100% (50000)	6M KOH	9.38 Wh kg <sup>-1</sup>	[110]
N-O GQDs	325 F g <sup>-1</sup> at 0.8 A g <sup>-1</sup>	82.6% (5000)	1M H <sub>2</sub> SO <sub>4</sub>	8.0 μWh cm <sup>-2</sup>	[111]





carbon-based MSCs. After 10,000 cycles, the initial capacity remains 89.2% (Fig. 4F), with good cycle stability.

#### 4 Photocatalytic Hydrogen Evolution Applications of Quantum Dots

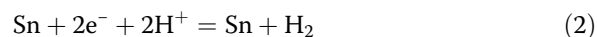
With the speediness expend of fossil fuels for the past few years and causing energy absence, environmental

contamination, and global warming, sustainable energy conversion appliance have progressively become common subjects of global Progress [118–120]. Utilize solar energy to convert water into hydrogen fuel is an effective way to resolve energy and environmental problems [121–125]. In terms of thermodynamics, an excellent hydrogen production photocatalyst needs to have a

conduction band (CB) position that is lower than the oxidation-reduction of  $H^+/H_2$  (0 V vs. NHE, pH = 0), and the valence band (VB) position is higher than the oxidation-reduction potential of  $O_2/H_2O$  (1.23V vs. NHE, pH=0) [126, 127]. However, the low quantum efficiency of conventional catalysts seriously hinders the large-scale application of photocatalytic water decomposition [128, 129]. Compared with bulk semiconductor materials, QDs generate multiple excitons due to quantum confinement, achieving better charge separation and transmission, and better improving photocatalytic activity [130, 131]. For example, Wu et al. prepared two-dimensional nanocrystals with catalytic activity by sandwiched monolayer  $WO_4$  between bilayer  $Bi_2O_3$  for photocatalytic hydrogen production, with  $H_2$  generation efficiency up to  $56.9 \mu\text{mol/g/h}$  [132]. By virtue of the excellent environmental stability and unique chemical, physical, electronic and optical properties of quantum dot materials, energy saving photocatalysts with higher performance can be obtained [133–136].

Researchers have successfully synthesized both boron (B) and phosphorus (P) co-doped silicon quantum dots (Si QDs) and tested the photocatalytic hydrogen production activity [137]. The study proved for the first time that the quantum size effect of prepared photocatalyst QDs has a significant impact on the photocatalytic  $H_2$  generation rate. The diameter of Si particles trails off, the rate of  $H_2$  generation aggrandizes sharply. Gao et al. [138] converted oil-soluble  $ZnxCd1-xS$  quantum dot (ZCS QDs) without photocatalytic activity into water-soluble ZCS quantum *via* ligand exchange and the synthesis process is shown in Fig. 5A. The TEM images (Fig. 5B) show that the ZCS quantum dots have excellent dispersibility and narrow size distribution of 4 nm. Under specific conditions, the water-soluble ZCS QDs exhibits splendid catalytic efficiency under visible light ( $1340 \mu\text{mol h}^{-1} \text{g}^{-1}$ ), 11.5 times more active than the oil-soluble QDs counterpart (Fig. 5C). On account of the small particle size, broad surface area feeds with excellent separation efficiency of photogenerated carriers, thereby improve the photocatalytic activity. Xiang et al. [139] used solvothermal method to prepare oil-soluble cadmium sulfide (CdS) quantum dots, and then successfully transferred them into water through ligand exchange (Fig. 5D). The photocatalytic hydrogen activity experimental result of the catalyst doped by  $Sn^{2+}$  reached  $1.94 \text{ mmol g}^{-1} \text{h}^{-1}$ , which is significantly higher than the original water-soluble CdS QDs ( $0.059 \text{ mmol g}^{-1} \text{h}^{-1}$ ). Further proposed reaction mechanism of photocatalytic hydrogen production indicated that  $Sn^{2+}$  ions were adsorbed on the surface of CdS quantum dots which can easily be reduced to  $Sn(0)$  by light (Fig. 5E). Therefore, the produced electrons and holes about as-prepared quantum dots can be separated and transferred

resultful, and the photocatalytic activity will largely enhance. The main reaction process is summarized as the following steps



So far, abundant and multifarious semiconductor materials have been used in photocatalytic hydrogen production [141–144]. Among them, cadmium sulfide (CdS) and carbon nitride ( $C_3N_4$ ) are excellent candidates owing to their narrow energy gap which can absorb the visible light, and the appropriate energy position can effectively reduce protons to  $H_2$  [145–149]. However, the photocatalytic hydrogen production of pure CdS and  $C_3N_4$  is extremely low due to the rapid recombination of photogenerated electrons and holes. To tackle such intrinsic problems, quantum dots are employed for boosting the charge separation efficiency, in order to enhance the photocatalytic hydrogen production performance.

Surface modification of the semiconductors by quantum dots is the most commonly used strategy to improve photocatalytic hydrogen production efficiency. Quantum dots can be used as co-catalysts to capture carriers, improving charge separation efficiency, reducing the energy barrier for hydrogen evolution, and serving as active sites in catalytic reactions. For example, Ma et al. [150] found the photocatalytic activity of CdS under visible light was greatly enhanced by the modification of novel nonmetallic  $Mo_2C$  QDs. The hydrogen evolution rate of the composite material (2.0%  $Mo_2C/CdS$ ) is  $172 \text{ mmol h}^{-1}$ , which is 10.21 times higher than the pure CdS. Liu et al. [151] creatively prepared the BP quantum dots bedecked on the surface of the CdS nanowires through a simple electrostatic self-assembly method. The resulting BPQDs/CdS composite material showed outstanding photocatalytic performance ( $9.9 \text{ mmol g}^{-1} \text{h}^{-1}$ ), 6.4 times higher than original CdS nanowires. The photocurrent and impedance test proved that the BPQDs/CdS composite interface can efficiently expedite the segregation and transfer of produced charge carriers. Li et al. [140] innovatively used  $Ti_3C_2$  QDs modified  $g-C_3N_4$  nanosheet *via* self-assembly method to prepare  $g-C_3N_4@Ti_3C_2$  composites (Fig. 5F). Photoluminescence (PL) test, photocurrent measurement as well as electrochemical impedance spectroscopy (EIS) experiment showed that as-prepared composites have superior carrier separation efficiency (Fig. 5G and H). The catalytic performance of  $g-C_3N_4@Ti_3C_2$  QD material ( $5123.8 \mu\text{mol g}^{-1} \text{h}^{-1}$ ) is 26.57 times higher compared with  $g-C_3N_4$  nanosheet ( $192.8 \mu\text{mol g}^{-1} \text{h}^{-1}$ ). Fig. 5I shows the photocatalytic reaction process of  $g-C_3N_4@Ti_3C_2$  QD composite material with mimetic solar irradiation. The

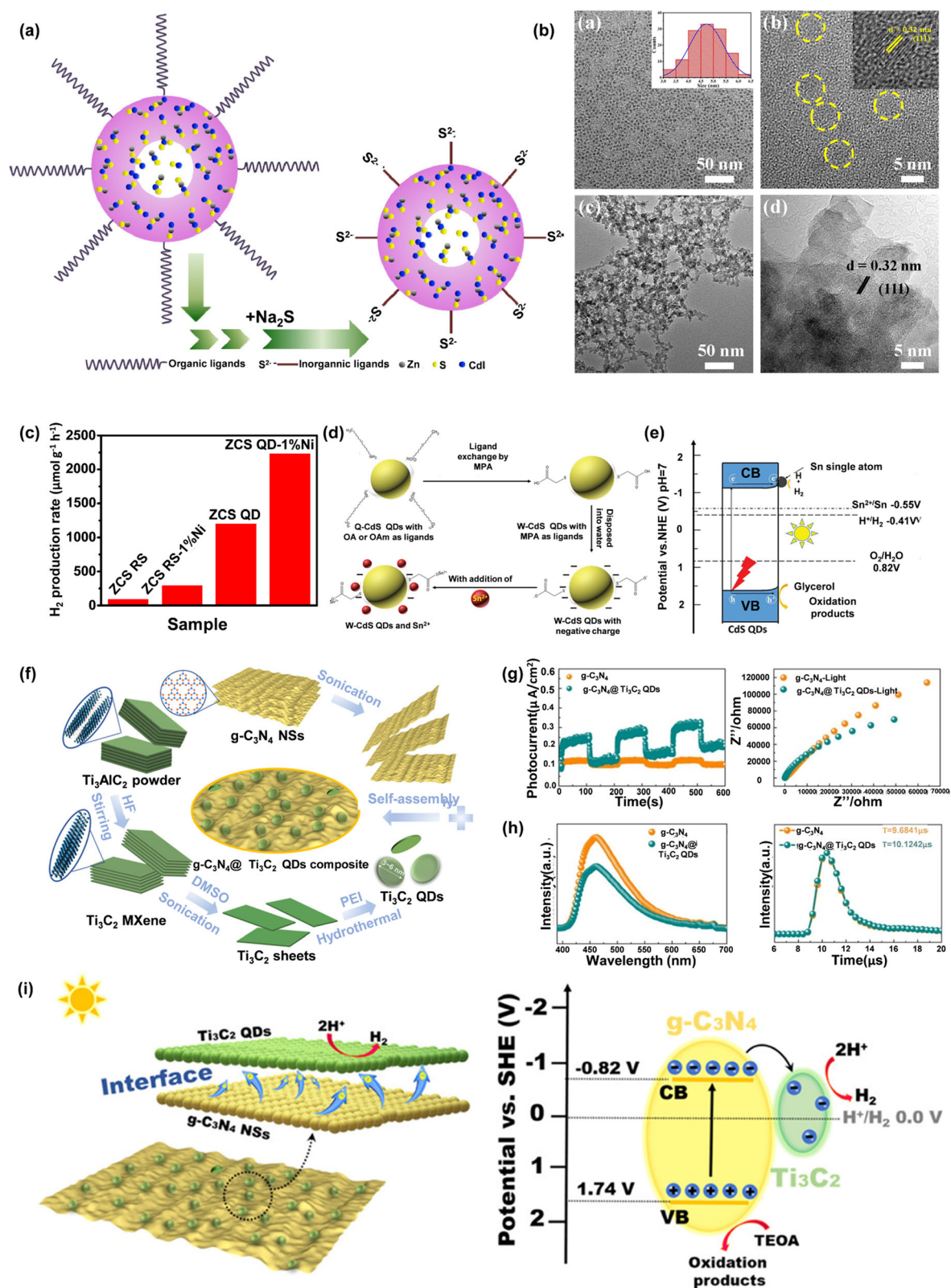


Fig. 5 (See legend on next page.)



(See figure on previous page.)

**Fig. 5** **A** The schematic illustration of the ligand-exchange process for ZCS QD; **B** The TEM images of ZCS quantum dots; **C** Photocatalytic  $\text{H}_2$ -production rates of ZCS RS, RS-1% Ni, QD, and QD-1% Ni; (Reprinted from Ref. [138]. Copyright 2021 Elsevier Ltd.) **D** A schematic illustration of ligand exchange and adsorption of  $\text{Sn}^{2+}$  on the surface of CdS QDs; **E**  $\text{H}_2$  production and separation of CdS QDs with  $\text{Sn}^{2+}$  or Sn atom under visible light irradiation; (Reprinted from Ref. [139]. Copyright 2020 Wiley-VCH.) **F** Schematic Illustration of the Preparation of  $\text{g-C}_3\text{N}_4/\text{Ti}_3\text{C}_2$  QD Composites; **G** Steady photoluminescence (PL) and time-resolved fluorescence decay spectra of  $\text{g-C}_3\text{N}_4$  and  $\text{g-C}_3\text{N}_4/\text{Ti}_3\text{C}_2$  QDs-100 mL composites,  $\lambda_{\text{ex}} = 325 \text{ nm}$ ; **H** Photocurrent responses and EIS of  $\text{g-C}_3\text{N}_4$  NSs and  $\text{g-C}_3\text{N}_4/\text{Ti}_3\text{C}_2$  QDs-100 mL composites; **I** Schematic Photocatalytic Mechanism of  $\text{g-C}_3\text{N}_4/\text{Ti}_3\text{C}_2$  QD Composites. (Reprinted from Ref. [140]. Copyright 2019 ACS Publications)

electrons on the surface produced by excitation of  $\text{g-C}_3\text{N}_4$  nanosheet can quickly migrate to  $\text{Ti}_3\text{C}_2$  QDs via  $\text{g-C}_3\text{N}_4\text{-Ti}_3\text{C}_2$  heterojunction due to the metallic nature of  $\text{Ti}_3\text{C}_2$  QDs. These electrons will then transfer to protons for hydrogen production on the active sites of  $\text{Ti}_3\text{C}_2$  QDs.

The preparation of heterojunction is a critical path to enhance photocatalytic activities owing to its ability to restrain the recombination of photo-generated carriers. Wang et al. [152] has successfully synthesized hexagonal  $\text{ZnIn}_2\text{S}_4$  microspheres, and then decorated the surface of unique  $\text{ZnIn}_2\text{S}_4$  microspheres by the cubic  $\text{ZnIn}_2\text{S}_4$  QDs using hydrothermal growth method (Fig. 6A). It can be seen from Fig. 6B that the abundant quantum dots are well dispersed on the surface of the nanosheet. HRTEM further proved the formation of heterogeneous junctions, where the lattice stripe with  $d$  spacing about 0.325 nm and 0.375 nm are assigned for (102) plane of H- $\text{ZnIn}_2\text{S}_4$  and (220) plane of C- $\text{ZnIn}_2\text{S}_4$  respectively. The as-prepared  $\text{ZnIn}_2\text{S}_4$  heterojunction material displays excellent photocatalytic performance ( $114.2 \mu\text{mol h}^{-1}$ ), which is 7.4 and 3.3 times better than pure cubic and hexagonal  $\text{ZnIn}_2\text{S}_4$  (Fig. 6C, D). The as-prepared unique  $\text{ZnIn}_2\text{S}_4$  heterojunction QDs material realizes the quick transfer and segregation of photogenerated carriers. In addition, the formed sulfur vacancies in heterogeneous junctions through quantum dots can furnish more electron capture sites for catalytic reduction reaction, thereby improving the photocatalytic activity. Shi et al. [154] fabricated a Z-scheme heterostructure material BP/RP-QD via wet-chemistry method owing to the quantum confinement effect. The concentration of cobalt ions added to the sample was determined by ICP-AES. The hydrogen production experiments confirm 2 wt% Co-BP/RP-QD has the highest activity ( $375 \mu\text{mol h}^{-1} \text{ g}^{-1}$ ), which is 10.41 and 3.94 times that of BP-QD ( $36 \mu\text{mol h}^{-1} \text{ g}^{-1}$ ) and RP-QD ( $95 \mu\text{mol h}^{-1} \text{ g}^{-1}$ ), indicating that the formation of a heterojunction photocatalyst can greatly improve photocatalytic hydrogen production activity. Based on their previous research, Jiao et al. [153] successfully synthesized a new type of ternary heterojunction material with  $\text{MoS}_2$  quantum dot uniformly dispersed in  $\text{g-C}_3\text{N}_4$  nanosheet/N-doped carbon dot.

The synthetic  $\text{g-C}_3\text{N}_4/\text{NCDS}/\text{MoS}_2$  material shows preeminent photocatalytic hydrogen evolution activity ( $226.35 \mu\text{mol g}^{-1} \text{ h}^{-1}$ ), 54 times higher than pure  $\text{g-C}_3\text{N}_4/\text{MoS}_2$ -3% (Fig. 6E). In addition, the as-prepared  $\text{g-C}_3\text{N}_4/\text{NCDS}/\text{MoS}_2$  exhibits outstanding light stability. The mechanism of  $\text{g-C}_3\text{N}_4/\text{NCDS}/\text{MoS}_2$  photocatalytic hydrogen production is proposed in Fig. 6F. Both  $\text{g-C}_3\text{N}_4$  and NCDS are excited to produce electron-hole pairs under visible light. The ternary heterojunction photocatalyst formed by doping  $\text{MoS}_2$  quantum dot can significantly accelerate the transfer and segregate of produced carriers, thereby heighten the performance of photocatalytic hydrogen production.

In this review, we have summarized the applications of QDs based nanomaterials in lithium- sulfur batteries, supercapacitors, and photocatalytic hydrogen production, with the emphasis on material preparation, structure, and energy storage properties. According to the unique physical and chemical properties of QDs and the current research progress, the important roles of QDs in energy storage and conversion system are listed as follows:

(1) Reducing the size of electrode material to QD level can greatly reduce the volume change stress, improve electrode dynamics, and shorten the migration distance of lithium ions, sodium ions, or other ions within the battery.

(2) QDs embedded in carbon electrode expands the distance between carbon atom layers, reduces the degree of order, forms heterojunctions, as well as enhances the storage capacity and diffusion rate of lithium ions. Higher SC properties can be obtained by increasing specific surface area and doping nitrogen on common carbon materials. The storage of electrolyte ions in deep holes is promoted, thus the rate and capacitance performance are significantly improved.

(3) Quantum dot modified semiconductor materials can be used as a cocatalyst to capture carriers, improve the charge separation efficiency of hydrogen evolution, and also as the active site of catalytic reaction, thus improving the overall performance of photocatalytic hydrogen production.

Many researchers have put effort into the synthesis methods of various QDs. Different design and assembly

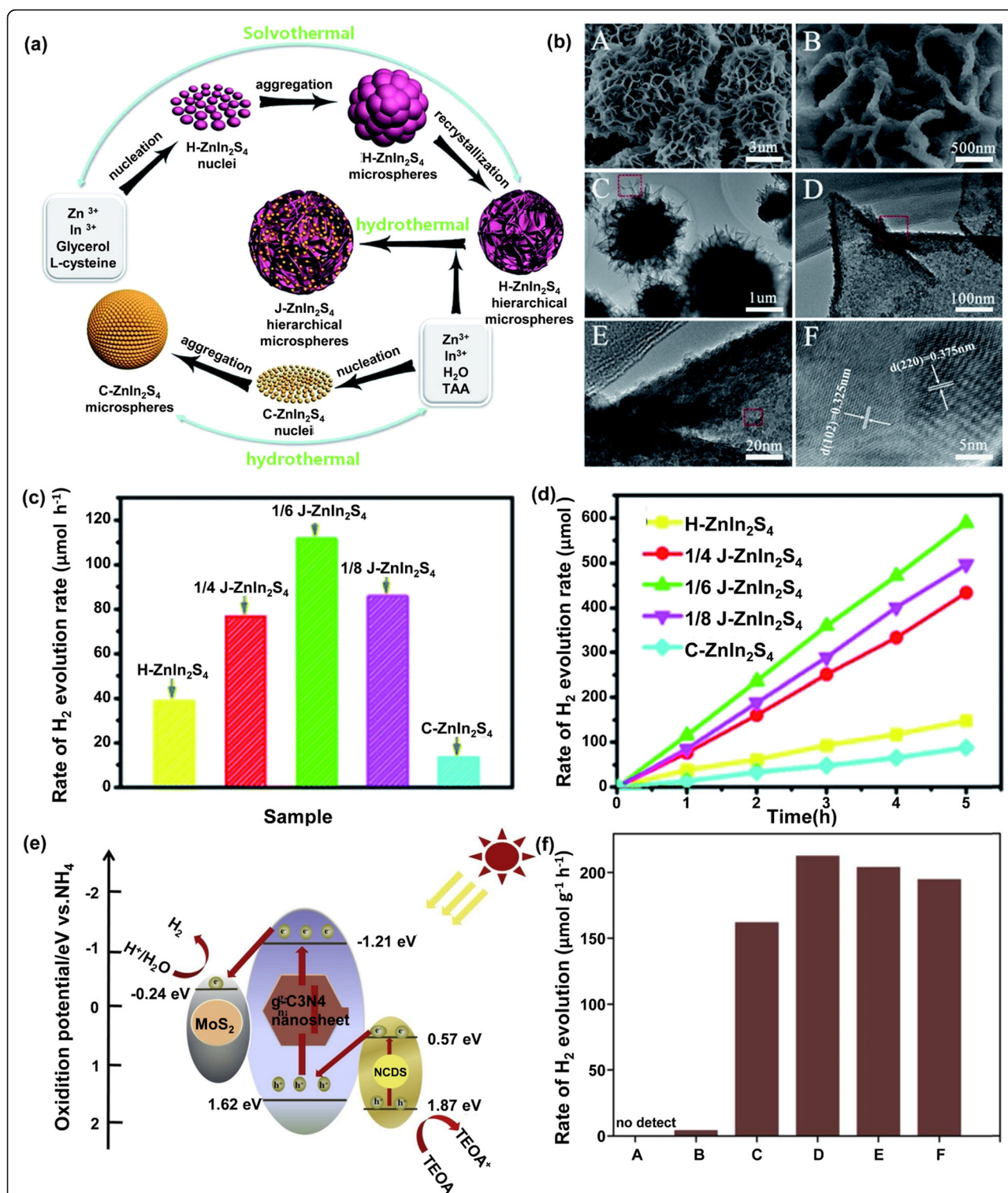


**Fig. 6** A Schematic illustration of the formation process of the cubic quantum dot/hexagonal microsphere  $\text{ZnIn}_2\text{S}_4$  heterophase junctions; B SEM images, TEM image, and the HRTEM image of the cubic quantum dot/hexagonal microsphere  $\text{ZnIn}_2\text{S}_4$  heterophase junction; C, D Comparison of the photocatalytic  $\text{H}_2$  evolution rate of  $\text{H-ZnIn}_2\text{S}_4$ ,  $\text{C-ZnIn}_2\text{S}_4$  and  $\text{J-ZnIn}_2\text{S}_4$  samples with different cubic/hexagonal mole ratios (1:4, 1:6, and 1:8) and different reaction times; (Reprinted from Ref. [152]. Copyright 2017 Royal Society of Chemistry.) E Proposed photocatalytic mechanism for hydrogen evolution over  $\text{g-C}_3\text{N}_4/\text{NCDS}/\text{MoS}_2$  under visible light irradiation; F Photocatalytic reaction of  $\text{g-C}_3\text{N}_4/\text{NCDS}/\text{MoS}_2$  composite photocatalyst under visible Light ( $\lambda \geq 420 \text{ nm}$ ) for 3 h. (A: bulk  $\text{g-C}_3\text{N}_4$ . B:  $\text{g-C}_3\text{N}_4/\text{MoS}_2$ -3%. C:  $\text{g-C}_3\text{N}_4/\text{NCDS}/\text{MoS}_2$ -2%. D:  $\text{g-C}_3\text{N}_4/\text{NCDS}/\text{MoS}_2$ -3%. E:  $\text{g-C}_3\text{N}_4/\text{NCDS}/\text{MoS}_2$ -4%. F:  $\text{g-C}_3\text{N}_4/\text{NCDS}/\text{MoS}_2$ -5%). (Reprinted from Ref. [153]. Copyright 2019 Elsevier Ltd.)

strategies to prepare advanced QD-based electrode materials are also established. However, there is still plenty of unsolved scientific and technical issues in the field before we can step into practical application:

(1) So far, the synthetic QDs/doped QDs strategy still has many limitations, such as low yield, synthetic complexity, and high cost, which hinder the further development and application. In addition, the polydisperse and reproducibility issue of QDs synthesis makes it difficult to ensure the stability of the electrode material in the cycle process. There is an urgent need to explore simple, economical, and efficient ways to produce high-quality QDs.

(2) The research of QDs composites in the field of electrochemical energy storage is still in the infancy stage. The scarcity of systematic research on the electrochemical behavior and energy storage mechanism of QDs and other components hinders us to understand the influence of various parameters of QDs on their performance in energy storage and conversion systems. In this case, it is imperative to conduct comprehensive studies on such topics eg. the interaction mechanism of QDs with other materials, and its influence on the properties of composite materials by both experiments and theoretical calculations.

(3) Graphene QDs has a large specific surface area and can be easily doped with transition metals and alkali metals, which can greatly improve hydrogen storage capacity. Therefore, graphene QDs is considered as a potential candidate material for solid-state hydrogen storage. However, the research on QDs hydrogen storage is almost blank, and only a few researchers try to dope Pb, [155] Cu, [69] Cr, [156] Li [70] and other metals in QDs to improve the performance of hydrogen storage. No QDs composite material for hydrogen storage has been prepared so far, which leaves us a promising but unexplored field.

In conclusion, this paper reviews the importance and great potential of quantum dot composites in the development of high-performance energy storage and catalytic systems. It is reasonable to conclude that QDs is becoming an important multifunctional material for energy storage/conversion devices. In particular, with the development of advanced technologies and characterization methods, new physicochemical properties of QDs will be discovered, which will lead to an extension of its application to other promising research fields. We can foresee that the research of advanced electrode materials based on QDs and their potential applications in energy-related fields will encounter an explosive growth in the near future.

#### Abbreviations

QDs: Quantum dots; RGO: Reduced graphene oxide; CQD: Carbon quantum dots; CTAB: Cetyltrimethylammonium bromide; PEI-Cdots: Polyethyleneimine

functionalized carbon dots; BP: Black phosphorus; BPQDs: BP quantum dots; SEM: Scanning electron microscope; HQDs: Heterostructure quantum dots; ALD: Atomic layer deposition; MQD: Mo<sub>2</sub>C quantum dot; NG: N-doped graphene; SCs: Supercapacitors; DLCs: Double-layer capacitors; GQDs: Graphene quantum dots; MSCs: Micro-supercapacitors; CB: Conduction band; VB: Valence band; ZCS QDs: ZnxCd1-xS quantum dot; CdS: Cadmium sulfide; PL: Photoluminescence; EIS: Electrochemical impedance spectroscopy

#### Acknowledgements

The authors acknowledge the financial support from the National Key Research and Development Program of China (2020YFC2005500), the National Natural Science Foundation of China (No. 81972901), Science Foundation of China University of Petroleum (No. 2462020YXZZ0188, 2462019QNXZ02, 2462018BJC004), the Academy of Finland (No. 330214) and the U.S. National Science Foundation (No. 2004251).

#### Code availability

Not applicable

#### Authors' contributions

In this manuscript, Quan Xu conceived and designed this work, Yingchun Niu, Jiapeng Li and Jiajia Gao wrote most of the manuscript, Lan Ding, Huiqin Ni, Peide Zhu, Yinping Liu and Yaoyao Tang helped with the picture collection. Zhong-Peng Lv, Bo Peng, Travis Shihao Hu, Hongjun Zhou and Chunming Xu helped with the manuscript polishing. All the authors approve this submission.

#### Funding

This work was supported by the National Key Research and Development Program of China (2020YFC2005500), the National Natural Science Foundation of China (No. 81972901), Science Foundation of China University of Petroleum (No. 2462020YXZZ0188, 2462019QNXZ02, 2462018BJC004), the Academy of Finland (No. 330214) and the U.S. National Science Foundation (No. 2004251).

#### Availability of data and materials

Not applicable

#### Declarations

#### Ethics approval and consent to participate

The authors agreed for consent to participate

#### Consent for publication

Its publication has been approved explicitly by all authors and the responsible authorities where the work was carried out.

#### Competing interests

The authors declare no conflict of interest and competing

#### Author details

<sup>1</sup>State Key Laboratory of Heavy Oil Processing, China University of Petroleum-Beijing, Beijing 102249, China. <sup>2</sup>Department of Applied Physics, Aalto University, FIN-00076 Aalto, Finland. <sup>3</sup>Department of Mechanical Engineering, California State University, Los Angeles, California 90032, United States.

Received: 5 October 2021 Accepted: 2 January 2022

Published online: 19 April 2022

#### References

1. Zhao N, You F (2020) Can renewable generation, energy storage and energy efficient technologies enable carbon neutral energy transition? *Appl Energy* 279:115889. <https://doi.org/10.1016/j.apenergy.2020.115889>
2. Czaun M, Kothandaraman J, Goepfert A, Yang B, Greenberg S, May RB, Olah GA, Prakash GKS (2016) Iridium-Catalyzed Continuous Hydrogen Generation from Formic Acid and Its Subsequent Utilization in a Fuel Cell: Toward a Carbon Neutral Chemical Energy Storage. *ACS Catal* 6:7475–7484. <https://doi.org/10.1021/acscatal.6b01605>



3. Ahirwar S, Mallick S, Bahadur D (2017) Electrochemical Method To Prepare Graphene Quantum Dots and Graphene Oxide Quantum Dots. *ACS Omega* 2:8343–8353. <https://doi.org/10.1021/acsomega.7b01539>
4. Penner RM (2000) Hybrid electrochemical/chemical synthesis of quantum dots. *Acc Chem Res* 33:78–86
5. Yang Y, Bremner S, Menictas C, Kay M (2018) Battery energy storage system size determination in renewable energy systems: A review. *Renew Sustain Energy Rev* 91:109–125
6. Denholm P, Nunemaker J, Gagnon P, Cole W (2020) The potential for battery energy storage to provide peaking capacity in the United States. *Renew Energy* 151:1269–1277
7. Ma T, Yang H, Lu L (2015) Development of hybrid battery–supercapacitor energy storage for remote area renewable energy systems. *Appl Energy* 153:56–62
8. Dubal DP, Ayyad O, Ruiz V, Gómez-Romero P (2015) Hybrid energy storage: the merging of battery and supercapacitor chemistries. *Chem Soc Rev* 44: 1777–1790. <https://doi.org/10.1039/C4CS00266K>
9. Samsudin MFR, Sufian S (2020) Hybrid 2D/3D g-C<sub>3</sub>N<sub>4</sub>/BiVO<sub>4</sub> photocatalyst decorated with RGO for boosted photoelectrocatalytic hydrogen production from natural lake water and photocatalytic degradation of antibiotics. *J Mol Liq* 314:113530. <https://doi.org/10.1016/j.molliq.2020.113530>
10. Adamopoulos PM, Papagiannis I, Raptis D, Lianos P (2019) Photoelectrocatalytic Hydrogen Production Using a TiO<sub>2</sub>/WO<sub>3</sub> Bilayer Photocatalyst in the Presence of Ethanol as a Fuel. *Catalysts* 9:976. <https://doi.org/10.3390/catal9120976>
11. Baker SN, Baker GA (2010) Luminescent Carbon Nanodots: Emergent Nanolights. *Angew Chem Int Ed* 49:6726–6744. <https://doi.org/10.1002/anie.200906623>
12. Fowley C, Nomikou N, McHale AP, McCaughan B, Callan JF (2013) Extending the tissue penetration capability of conventional photosensitisers: a carbon quantum dot–protoporphyrin IX conjugate for use in two-photon excited photodynamic therapy. *Chem Commun* 49:8934–8936. <https://doi.org/10.1039/C3CC45181J>
13. Wu P, Xu Y, Zhan J, Li Y, Xue H, Pang H (2018) The research development of quantum dots in electrochemical energy storage. *Small* 14:1801479
14. Wang J, Tang L, Zeng G, Deng Y, Dong H, Liu Y, Wang L, Peng B, Zhang C, Chen F (2018) 0D/2D interface engineering of carbon quantum dots modified Bi<sub>2</sub>WO<sub>6</sub> ultrathin nanosheets with enhanced photoactivity for full spectrum light utilization and mechanism insight. *Appl Catal B Environ* 222: 115–123
15. Molaei MJ (2019) Carbon quantum dots and their biomedical and therapeutic applications: a review. *RSC Adv* 9:6460–6481
16. Ahmad P, Khandaker MU, Muhammad N, Khan G, Rehman F, Khan AS, Ullah Z, Khan A, Ali H, Ahmed SM, Rauf Khan MA, Iqbal J, Khan AA, Irshad MI (2019) Fabrication of hexagonal boron nitride quantum dots via a facile bottom-up technique. *Ceram Int* 45:22765–22768. <https://doi.org/10.1016/j.ceramint.2019.07.316>
17. Yang J, Ling T, Wu W-T, Liu H, Gao M-R, Ling C, Li L, Du X-W (2013) A top-down strategy towards monodisperse colloidal lead sulphide quantum dots. *Nat Commun* 4:1–6
18. Sun H, Ji H, Ju E, Guan Y, Ren J, Qu X (2015) Synthesis of Fluorinated and Nonfluorinated Graphene Quantum Dots through a New Top-Down Strategy for Long-Time Cellular Imaging. *Chem Eur J* 21:3791–3797
19. Yan Y, Zhai D, Liu Y, Gong J, Chen J, Zan P, Zeng Z, Li S, Huang W, Chen P (2020) van der Waals Heterojunction between a Bottom-Up Grown Doped Graphene Quantum Dot and Graphene for Photoelectrochemical Water Splitting. *ACS Nano* 14:1185–1195. <https://doi.org/10.1021/acsnano.9b09554>
20. Derivishi E, Ji Z, Htoon H, Sykora M, Doorn SK (2019) Raman spectroscopy of bottom-up synthesized graphene quantum dots: size and structure dependence. *Nanoscale* 11:16571–16581
21. Gao T, Wang X, Zhao J, Jiang P, Jiang F-L, Liu Y (2020) Bridge between temperature and light: bottom-up synthetic route to structure-defined graphene quantum dots as a temperature probe in vitro and in cells. *ACS Appl Mater Interfaces* 12:22002–22011
22. Beke D, Szekrényes Z, Balogh I, Czirágy Z, Kamarás K, Gali A (2013) Preparation of small silicon carbide quantum dots by wet chemical etching. *J Mater Res* 28:44–49. <https://doi.org/10.1557/jmr.2012.223>
23. Wu P, Yan X-P (2010) A simple chemical etching strategy to generate “ion-imprinted” sites on the surface of quantum dots for selective fluorescence turn-on detecting of metal ions. *Chem Commun* 46:7046–7048
24. Luo X, Guo B, Wang L, Deng F, Qi R, Luo S, Au C (2014) Synthesis of magnetic ion-imprinted fluorescent CdTe quantum dots by chemical etching and their visualization application for selective removal of Cd (II) from water. *Colloids Surf Physicochem Eng Asp* 462:186–193
25. Duan J, Song L, Zhan J (2009) One-pot synthesis of highly luminescent CdTe quantum dots by microwave irradiation reduction and their Hg<sub>2</sub>+ sensitive properties. *Nano Res* 2:61–68. <https://doi.org/10.1007/s12274-009-9004-0>
26. Qian H, Li L, Ren J (2005) One-step and rapid synthesis of high quality alloyed quantum dots (CdSe–CdS) in aqueous phase by microwave irradiation with controllable temperature. *Mater Res Bull* 40:1726–1736
27. Omer KM, Aziz KHH, Salih YM, Tofiq DI, Hassan AQ (2019) Photoluminescence enhancement via microwave irradiation of carbon quantum dots derived from solvothermal synthesis of L-arginine. *New J Chem* 43:689–695
28. Dang H, Huang L-K, Zhang Y, Wang C-F, Chen S (2016) Large-Scale Ultrasonic Fabrication of White Fluorescent Carbon Dots. *Ind Eng Chem Res* 55:5335–5341. <https://doi.org/10.1021/acs.iecr.6b00894>
29. Huang H, Cui Y, Liu M, Chen J, Wan Q, Wen Y, Deng F, Zhou N, Zhang X, Wei Y (2018) A one-step ultrasonic irradiation assisted strategy for the preparation of polymer-functionalized carbon quantum dots and their biological imaging. *J Colloid Interface Sci* 532:767–773
30. Hao J, Tai G, Zhou J, Wang R, Hou C, Guo W (2020) Crystalline semiconductor boron quantum dots. *ACS Appl Mater Interfaces* 12:17669–17675
31. Li Y, Hu Y, Zhao Y, Shi G, Deng L, Hou Y, Qu L (2011) An electrochemical avenue to green-luminescent graphene quantum dots as potential electron-acceptors for photovoltaics. *Adv Mater* 23:776–780
32. Xu M, Li Z, Zhu X, Hu N, Wei H, Yang Z, Zhang Y (2013) Hydrothermal/Solvothermal Synthesis of Graphene Quantum Dots and Their Biological Applications. *Nano Biomed Eng* 5:65–71
33. Ren X, Wei Q, Ren P, Wang Y, Peng Y (2018) Hydrothermal-solvothermal cutting integrated synthesis and optical properties of MoS<sub>2</sub> quantum dots. *Opt Mater* 86:62–65
34. Mozdabar A, Nouralishahi A, Fatemi S, Mirakhori G (2018) The effect of precursor on the optical properties of carbon quantum dots synthesized by hydrothermal/solvothermal method. AIP Publishing LLC, Melville
35. Sun Y-P, Zhou B, Lin Y, Wang W, Fernando KAS, Pathak P, Mezzani MJ, Harruff BA, Wang X, Wang H, Luo PG, Yang H, Kose ME, Chen B, Veca LM, Xie S-Y (2006) Quantum-Sized Carbon Dots for Bright and Colorful Photoluminescence. *J Am Chem Soc* 128:7756–7757. <https://doi.org/10.1021/ja062677d>
36. Shen J, Zhu Y, Chen C, Yang X, Li C (2011) Facile preparation and upconversion luminescence of graphene quantum dots. *Chem Commun* 47:2580–2582
37. Zhou C, Jiang W, Via BK (2014) Facile synthesis of soluble graphene quantum dots and its improved property in detecting heavy metal ions. *Colloids Surf B Biointerfaces* 118:72–76
38. Xu Q, Cai W, Li W, Sreeprasad TS, He Z, Ong W-J, Li N (2018) Two-dimensional quantum dots: Fundamentals, photoluminescence mechanism and their energy and environmental applications. *Mater Today Energy* 10: 222–240. <https://doi.org/10.1016/j.mtener.2018.09.005>
39. Tian L, Yang S, Yang Y, Li J, Deng Y, Tian S, He P, Ding G, Xie X, Wang Z (2016) Green, simple and large scale synthesis of N-doped graphene quantum dots with uniform edge groups by electrochemical bottom-up synthesis. *RSC Adv* 6:82648–82653
40. Hang D-R, Sun D-Y, Chen C-H, Wu H-F, Chou MM, Islam SE, Sharma KH (2019) Facile bottom-up preparation of WS<sub>2</sub>-based water-soluble quantum dots as luminescent probes for hydrogen peroxide and glucose. *Nanoscale Res Lett* 14:1–15
41. Xu N, Li H, Gan Y, Chen H, Li W, Zhang F, Jiang X, Shi Y, Liu J, Wen Q, Zhang H (2020) Zero-Dimensional MXene-Based Optical Devices for Ultrafast and Ultranarrow Photonics Applications. *Adv Sci* 7:2002209. <https://doi.org/10.1002/advs.202002209>
42. Lu H, Li W, Dong H, Wei M (2019) Graphene Quantum Dots for Optical Bioimaging. *Small* 15:1902136. <https://doi.org/10.1002/smll.201902136>
43. Liu Q, Sun J, Gao K, Chen N, Sun X, Ti D, Bai C, Cui R, Qu L (2020) Graphene quantum dots for energy storage and conversion: from fabrication to applications. *Mater Chem Front* 4:421–436. <https://doi.org/10.1039/C9QM00553F>

44. Wang G, Zhang L, Zhang J (2012) A review of electrode materials for electrochemical supercapacitors. *Chem Soc Rev* 41:797–828. <https://doi.org/10.1039/C1CS15060J>
45. Li B, Dai F, Xiao Q, Yang L, Shen J, Zhang C, Cai M (2016) Nitrogen-doped activated carbon for a high energy hybrid supercapacitor. *Energy Environ Sci* 9:102–106. <https://doi.org/10.1039/C5EE03149D>
46. Armand M, Tarascon J-M (2008) Building better batteries. *Nature* 451:652–657. <https://doi.org/10.1038/451652a>
47. Zhao Z, Xie Y (2017) Enhanced electrochemical performance of carbon quantum dots-polyaniline hybrid. *J Power Sources* 337:54–64. <https://doi.org/10.1016/j.jpowsour.2016.10.110>
48. Liu W-W, Feng Y-Q, Yan X-B, Chen J-T, Xue Q-J (2013) Superior Micro-Supercapacitors Based on Graphene Quantum Dots. *Adv Funct Mater* 23: 4111–4122. <https://doi.org/10.1002/adfm.201203771>
49. Li J, Yun X, Hu Z, Xi L, Li N, Tang H, Lu P, Zhu Y (2019) Three-dimensional nitrogen and phosphorus co-doped carbon quantum dots/reduced graphene oxide composite aerogels with a hierarchical porous structure as superior electrode materials for supercapacitors. *J Mater Chem A* 7:26311–26325
50. Li Z, Bu F, Wei J, Yao W, Wang L, Chen Z, Pan D, Wu M (2018) Boosting the energy storage densities of supercapacitors by incorporating N-doped graphene quantum dots into cubic porous carbon. *Nanoscale* 10:22871–22883
51. Tan H, Cho H-W, Wu J-J (2018) Binder-free ZnO@ZnSnO<sub>3</sub> quantum dots core-shell nanorod array anodes for lithium-ion batteries. *J Power Sources* 388:11–18. <https://doi.org/10.1016/j.jpowsour.2018.03.066>
52. Wang B, Xie Y, Liu T, Luo H, Wang B, Wang C, Wang L, Wang D, Dou S, Zhou Y (2017) LiFePO<sub>4</sub> quantum-dots composite synthesized by a general microreactor strategy for ultra-high-rate lithium ion batteries. *Nano Energy* 42:363–372. <https://doi.org/10.1016/j.nanoen.2017.11.040>
53. Huang S, Wang M, Jia P, Wang B, Zhang J, Zhao Y (2019) N-graphene motivated SnO<sub>2</sub>@SnS<sub>2</sub> heterostructure quantum dots for high performance lithium/sodium storage. *Energy Storage Mater* 20:225–233. <https://doi.org/10.1016/j.jensm.2018.11.024>
54. Li X, Hu K, Tang R, Zhao K, Ding Y (2016) CuS quantum dot modified carbon aerogel as an immobilizer for lithium polysulfides for high-performance lithium-sulfur batteries. *RSC Adv* 6:71319–71327. <https://doi.org/10.1039/C6RA11990E>
55. Chakrabarty N, Dey A, Krishnamurthy S, Chakraborty AK (2021) CeO<sub>2</sub>/Ce<sub>2</sub>O<sub>3</sub> quantum dot decorated reduced graphene oxide nanohybrid as electrode for supercapacitor. *Appl Surf Sci* 536:147960. <https://doi.org/10.1016/j.apsusc.2020.147960>
56. Sun J, Sun Y, Oh JAS, Gu Q, Zheng W, Goh M, Zeng K, Cheng Y, Lu L (2021) Insight into the structure-capacity relationship in biomass derived carbon for high-performance sodium-ion batteries. *J Energy Chem* 62:497–504. <https://doi.org/10.1016/j.jechem.2021.04.009>
57. Liu S, Cao X, Zhang Y, Wang K, Su Q, Chen J, He Q, Liang S, Cao G, Pan A (2020) Carbon quantum dot modified Na<sub>3</sub>V<sub>2</sub>(PO<sub>4</sub>)<sub>2</sub>F<sub>3</sub> as a high-performance cathode material for sodium-ion batteries. *J Mater Chem A* 8: 18872–18879. <https://doi.org/10.1039/D0TA04307A>
58. Sun J, Tu W, Chen C, Pleva A, Ye H, Sam Oh JA, He L, Wu T, Zeng K, Lu L (2019) Chemical Bonding Construction of Reduced Graphene Oxide-Anchored Few-Layer Bismuth Oxychloride for Synergistically Improving Sodium-Ion Storage. *Chem Mater* 31:7311–7319. <https://doi.org/10.1021/acs.chemmater.9b01828>
59. Sun J, Ye H, Oh JAS, Pleva A, Sun Y, Wu T, Sun Q, Zeng K, Lu L (2021) Elevating the discharge plateau of prussian blue analogs through low-spin Fe redox induced intercalation pseudocapacitance. *Energy Storage Mater* 43:182–189. <https://doi.org/10.1016/j.jensm.2021.09.004>
60. Shi R, Li Z, Yu H, Shang L, Zhou C, Waterhouse GIN, Wu L-Z, Zhang T (2017) Effect of Nitrogen Doping Level on the Performance of N-Doped Carbon Quantum Dot/TiO<sub>2</sub> Composites for Photocatalytic Hydrogen Evolution. *Chem Sus Chem* 10:4650–4656. <https://doi.org/10.1002/cssc.201700943>
61. Cao Y, Zhou H, Qian R-C, Liu J, Ying Y-L, Long Y-T (2017) Analysis of the electron transfer properties of carbon quantum dots on gold nanorod surfaces via plasmonic resonance scattering spectroscopy. *Chem Commun* 53:5729–5732. <https://doi.org/10.1039/C7CC01464C>
62. Liu J, Liu Y, Liu N, Han Y, Zhang X, Huang H, Lifshitz Y, Lee S-T, Zhong J, Kang Z (2015) Metal-free efficient photocatalyst for stable visible water splitting via a two-electron pathway. *Science* 347:970–974
63. Dai L (2017) Carbon-based catalysts for metal-free electrocatalysis. *Curr Opin Electrochem* 4:18–25. <https://doi.org/10.1016/j.coelec.2017.06.004>
64. Xie S, Zhang Q, Liu G, Wang Y (2016) Photocatalytic and photoelectrocatalytic reduction of CO<sub>2</sub> using heterogeneous catalysts with controlled nanostructures. *Chem Commun* 52:35–59. <https://doi.org/10.1039/C5CC07613G>
65. Cho J, Suwandaratne NS, Razek S, Choi Y-H, Piper LFJ, Watson DF, Banerjee S (2020) Elucidating the Mechanistic Origins of Photocatalytic Hydrogen Evolution Mediated by MoS<sub>2</sub>/CdS Quantum-Dot Heterostructures. *ACS Appl Mater Interfaces* 12:43728–43740. <https://doi.org/10.1021/acsami.0c12583>
66. Lu S-M, Li Y-J, Zhang J-F, Wang Y, Ying Y-L, Long Y-T (2019) Monitoring hydrogen evolution reaction catalyzed by MoS<sub>2</sub> quantum dots on a single nanoparticle electrode. *Anal Chem* 91:10361–10365
67. Enright MJ, Gilbert-Bass K, Sarsito H, Cossairt BM (2019) Photolytic C–O Bond Cleavage with Quantum Dots. *Chem Mater* 31:2677–2682
68. Elsayed MH, Jayakumar J, Abdellah M, Mansoure TH, Zheng K, Elewa AM, Chang C-L, Ting L-Y, Lin W-C, Yu H, Wang W-H, Chung C-C, Chou H-H (2021) Visible-light-driven hydrogen evolution using nitrogen-doped carbon quantum dot-implanted polymer dots as metal-free photocatalysts. *Appl Catal B Environ* 283:119659. <https://doi.org/10.1016/j.apcatb.2020.119659>
69. Malček M, Bučinský L (2020) On the hydrogen storage performance of Cu-doped and Cu-decorated graphene quantum dots: a computational study. *Theor Chem Acc* 139:167. <https://doi.org/10.1007/s00214-020-02680-2>
70. Tachikawa H, Iyama T (2019) Mechanism of Hydrogen Storage in the Graphene Nanoflake–Lithium–H<sub>2</sub> System. *J Phys Chem C* 123:8709–8716. <https://doi.org/10.1021/acs.jpcc.9b01152>
71. Manthiram A, Fu Y, Su Y-S (2013) Challenges and Prospects of Lithium–Sulfur Batteries. *Acc Chem Res* 46:1125–1134. <https://doi.org/10.1021/ar300179v>
72. Cai D, Wang L, Li L, Zhang Y, Li J, Chen D, Tu H, Han W (2019) Self-assembled CdS quantum dots in carbon nanotubes: induced polysulfide trapping and redox kinetics enhancement for improved lithium–sulfur battery performance. *J Mater Chem A* 7:806–815. <https://doi.org/10.1039/C8TA09906E>
73. Zhang Q, Sun C, Fan L, Zhang N, Sun K (2019) Iron fluoride vertical nanosheets array modified with graphene quantum dots as long-life cathode for lithium ion batteries. *Chem Eng J* 371:245–251. <https://doi.org/10.1016/j.cej.2019.04.073>
74. Ke G, Chen H, He J, Wu X, Gao Y, Li Y, Mi H, Zhang Q, He C, Ren X (2021) Ultrathin MoS<sub>2</sub> anchored on 3D carbon skeleton containing SnS quantum dots as a high-performance anode for advanced lithium ion batteries. *Chem Eng J* 403:126251. <https://doi.org/10.1016/j.cej.2020.126251>
75. Ding H, Zhang Q, Liu Z, Wang J, Ma R, Fan L, Wang T, Zhao J, Ge J, Lu X, Yu X, Lu B (2018) TiO<sub>2</sub> quantum dots decorated multi-walled carbon nanotubes as the multifunctional separator for highly stable lithium sulfur batteries. *Electrochimica Acta* 284:314–320. <https://doi.org/10.1016/j.electacta.2018.07.167>
76. Wang J, Wang Z, Zhu Z (2017) Synergetic effect of Ni(OH)<sub>2</sub> cocatalyst and CNT for high hydrogen generation on CdS quantum dot sensitized TiO<sub>2</sub> photocatalyst. *Appl Catal B Environ* 204:577–583. <https://doi.org/10.1016/j.apcatb.2016.12.008>
77. Cao A, Liu Z, Chu S, Wu M, Ye Z, Cai Z, Chang Y, Wang S, Gong Q, Liu Y (2010) A Facile One-step Method to Produce Graphene–CdS Quantum Dot Nanocomposites as Promising Optoelectronic Materials. *Adv Mater* 22:103–106. <https://doi.org/10.1002/adma.200901920>
78. Liang X, Garsuch A, Nazar LF (2015) Sulfur cathodes based on conductive MXene nanosheets for high-performance lithium–sulfur batteries. *Angew Chem* 127:3979–3983
79. Wild M, O'Neill L, Zhang T, Purkayastha R, Minton G, Marinescu M, Offer GJ (2015) Lithium sulfur batteries, a mechanistic review. *Energy Environ Sci* 8: 3477–3494. <https://doi.org/10.1039/C5EE01388G>
80. Pang Q, Liang X, Kwok CY, Nazar LF (2016) Advances in lithium–sulfur batteries based on multifunctional cathodes and electrolytes. *Nat Energy* 1: 16132. <https://doi.org/10.1038/nenergy.2016.132>
81. Xu Z-L, Lin S, Onofrio N, Zhou L, Shi F, Lu W, Kang K, Zhang Q, Lau SP (2018) Exceptional catalytic effects of black phosphorus quantum dots in shuttling-free lithium sulfur batteries. *Nat Commun* 9:4164. <https://doi.org/10.1038/s41467-018-06629-9>
82. Gao X-T, Xie Y, Zhu X-D, Sun K-N, Xie X-M, Liu Y-T, Yu J-Y, Ding B (2018) Ultrathin MXene Nanosheets Decorated with TiO<sub>2</sub> Quantum Dots as an

- Efficient Sulfur Host toward Fast and Stable Li-S Batteries. *Small* 14:1802443. <https://doi.org/10.1002/sml.201802443>
83. Hu Y, Chen W, Lei T, Zhou B, Jiao Y, Yan Y, Du X, Huang J, Wu C, Wang X, Wang Y, Chen B, Xu J, Wang C, Xiong J (2019) Carbon Quantum Dots-Modified Interfacial Interactions and Ion Conductivity for Enhanced High Current Density Performance in Lithium-Sulfur Batteries. *Adv Energy Mater* 9:1802955. <https://doi.org/10.1002/aenm.201802955>
84. Li W, Yang Y, Zhang G, Zhang Y-W (2015) Ultrafast and Directional Diffusion of Lithium in Phosphorene for High-Performance Lithium-Ion Battery. *Nano Lett* 15:1691–1697. <https://doi.org/10.1021/nl504336h>
85. Sun J, Sun Y, Pasta M, Zhou G, Li Y, Liu W, Xiong F, Cui Y (2016) Entrapment of Polysulfides by a Black-Phosphorus-Modified Separator for Lithium-Sulfur Batteries. *Adv Mater* 28:9797–9803. <https://doi.org/10.1002/adma.201602172>
86. Zhang Z, Lai Y, Zhang Z, Zhang K, Li J (2014) Al<sub>2</sub>O<sub>3</sub>-coated porous separator for enhanced electrochemical performance of lithium sulfur batteries. *Electrochimica Acta* 129:55–61. <https://doi.org/10.1016/j.electacta.2014.02.077>
87. Liu J, Yuan L, Yuan K, Li Z, Hao Z, Xiang J, Huang Y (2016) SnO<sub>2</sub> as a high-efficiency polysulfide trap in lithium-sulfur batteries. *Nanoscale* 8:13638–13645. <https://doi.org/10.1039/C6NR02345B>
88. Pang Y, Wei J, Wang Y, Xia Y (2018) Synergetic Protective Effect of the Ultralight MWCNTs/NCQDs Modified Separator for Highly Stable Lithium-Sulfur Batteries. *Adv Energy Mater* 8:1702288. <https://doi.org/10.1002/aenm.201702288>
89. Yu B, Chen D, Wang Z, Qi F, Zhang X, Wang X, Hu Y, Wang B, Zhang W, Chen Y, He J, He W (2020) Mo<sub>2</sub>C quantum dots@graphene functionalized separator toward high-current-density lithium metal anodes for ultrastable Li-S batteries. *Chem Eng J* 399:125837. <https://doi.org/10.1016/j.cej.2020.125837>
90. Chung S-H, Manthiram A (2014) High-Performance Li-S Batteries with an Ultra-lightweight MWCNT-Coated Separator. *J Phys Chem Lett* 5:1978–1983. <https://doi.org/10.1021/jz5006913>
91. Liu Y, Liu Q, Xin L, Liu Y, Yang F, Stach EA, Xie J (2017) Making Li-metal electrodes rechargeable by controlling the dendrite growth direction. *Nat Energy* 2:17083. <https://doi.org/10.1038/energy.2017.83>
92. Lin D, Liu Y, Cui Y (2017) Reviving the lithium metal anode for high-energy batteries. *Nat Nanotechnol* 12:194–206. <https://doi.org/10.1038/nnano.2017.16>
93. Ye H, Sun J, Zhang S, Lin H, Zhang T, Yao Q, Lee JY (2019) Stepwise Electrocatalysis as a Strategy against Polysulfide Shuttling in Li-S Batteries. *ACS Nano* 13:14208–14216. <https://doi.org/10.1021/acs.nano.9b07121>
94. Jia H, Cai Y, Lin J, Liang H, Qi J, Cao J, Feng J, Fei W (2018) Heterostructural Graphene Quantum Dot/MnO<sub>2</sub> Nanosheets toward High-Potential Window Electrodes for High-Performance Supercapacitors. *Adv Sci* 5:1700887. <https://doi.org/10.1002/advs.201700887>
95. Zahir N, Magri P, Luo W, Gaumet J-J, Pierrat P (2021) Recent Advances on Graphene Quantum Dots for Electrochemical Energy Storage Devices. *Energy Environ Mater* 5:201–214. <https://doi.org/10.1002/eem2.12167>
96. Noori A, El-Kady MF, Rahmanifar MS, Kaner RB, Mousavi MF (2019) Towards establishing standard performance metrics for batteries, supercapacitors and beyond. *Chem Soc Rev* 48:1272–1341. <https://doi.org/10.1039/C8CS00581H>
97. Qing Y, Jiang Y, Lin H, Wang L, Liu A, Cao Y, Sheng R, Guo Y, Fan C, Zhang S, Jia D, Fan Z (2019) Boosting the supercapacitor performance of activated carbon by constructing overall conductive networks using graphene quantum dots. *J Mater Chem A* 7:6021–6027. <https://doi.org/10.1039/C8TA11620B>
98. Ren K, Liu Z, Wei T, Fan Z (2021) Recent Developments of Transition Metal Compounds-Carbon Hybrid Electrodes for High Energy/Power Supercapacitors. *Nano-Micro Lett* 13:129–160. <https://doi.org/10.1007/s40820-021-00642-2>
99. Zhang R, Shen W, Zhong M, Zhang J, Guo S (2021) Carbon Nanofibers Cross-Linked and Decorated with Graphene Quantum Dots as Binder-Free Electrodes for Flexible Supercapacitors. *J Phys Chem C* 125:143–151. <https://doi.org/10.1021/acs.jpcc.0c08803>
100. Zhao J, Zhu J, Li Y, Wang L, Dong Y, Jiang Z, Fan C, Cao Y, Sheng R, Liu A, Zhang S, Song H, Jia D, Fan Z (2020) Graphene Quantum Dot Reinforced Electrospun Carbon Nanofiber Fabrics with High Surface Area for Ultrahigh Rate Supercapacitors. *ACS Appl Mater Interfaces* 12:11669–11678. <https://doi.org/10.1021/acsami.9b22408>
101. Liu Y, Roy S, Sarkar S, Xu J, Zhao Y, Zhang J (2021) A review of carbon dots and their composite materials for electrochemical energy technologies. *Carbon Energy* 3:795–826. <https://doi.org/10.1002/cey2.134>
102. Zhang YDJZS, Fan Z (2020) Application of Carbon-/Graphene Quantum Dots for Supercapacitors. *Acta Phys Chim Sin* 36:1903052
103. Kharangarh PR, Ravindra NM, Rawal R, Singh A, Gupta V (2021) Graphene quantum dots decorated on spinel nickel cobaltite nanocomposites for boosting supercapacitor electrode material performance. *J Alloys Compd* 876:159990. <https://doi.org/10.1016/j.jallcom.2021.159990>
104. Qi F, Shao L, Shi X, Wu F, Huang H, Sun Z, Trukhanov A (2021) "Carbon quantum dots-glue" enabled high-capacitance and highly stable nickel sulphide nanosheet electrode for supercapacitors. *J Colloid Interface Sci* 601:669–677. <https://doi.org/10.1016/j.jcis.2021.05.099>
105. Ji Z, Ma D, Dai W, Liu K, Shen X, Zhu G, Nie Y, Pasang D, Yuan A (2021) Anchoring nitrogen-doped carbon quantum dots on nickel carbonate hydroxide nanosheets for hybrid supercapacitor applications. *J Colloid Interface Sci* 590:614–621. <https://doi.org/10.1016/j.jcis.2021.01.102>
106. Zhu Y, Wu Z, Jing M, Hou H, Yang Y, Zhang Y, Yang X, Song W, Jia X, Ji X (2015) Porous NiCo<sub>2</sub>O<sub>4</sub> spheres tuned through carbon quantum dots utilised as advanced materials for an asymmetric supercapacitor. *J Mater Chem A* 3:866–877. <https://doi.org/10.1039/C4TA05507A>
107. Ganganboina AB, Park EY, Doong R-A (2020) Boosting the energy storage performance of V<sub>2</sub>O<sub>5</sub> nanosheets by intercalating conductive graphene quantum dots. *Nanoscale* 12:16944–16955. <https://doi.org/10.1039/D0NR04362A>
108. Wei J-S, Song T-B, Zhang P, Zhu Z-Y, Dong X-Y, Niu X-Q, Xiong H-M (2020) Integrating Carbon Dots with Porous Hydrogels to Produce Full Carbon Electrodes for Electric Double-Layer Capacitors. *ACS Appl Energy Mater* 3: 6907–6914. <https://doi.org/10.1021/acs.aem.0c00990>
109. Lv H, Gao X, Xu Q, Liu H, Wang Y-G, Xia Y (2017) Carbon Quantum Dot-Induced MnO<sub>2</sub> Nanowire Formation and Construction of a Binder-Free Flexible Membrane with Excellent Superhydrophilicity and Enhanced Supercapacitor Performance. *ACS Appl Mater Interfaces* 9:40394–40403. <https://doi.org/10.1021/acsami.7b14761>
110. Zhang S, Zhu J, Qing Y, Wang L, Zhao J, Li J, Tian W, Jia D, Fan Z (2018) Ultramicroporous Carbons Puzzled by Graphene Quantum Dots: Integrated High Gravimetric, Volumetric, and Areal Capacitances for Supercapacitors. *Adv Funct Mater* 28:1805898. <https://doi.org/10.1002/adfm.201805898>
111. Li Z, Cao L, Qin P, Liu X, Chen Z, Wang L, Pan D, Wu M (2018) Nitrogen and oxygen co-doped graphene quantum dots with high capacitance performance for micro-supercapacitors. *Carbon* 139:67–75. <https://doi.org/10.1016/j.carbon.2018.06.042>
112. Luo P, Guan X, Yu Y, Li X, Yan F (2019) Hydrothermal Synthesis of Graphene Quantum Dots Supported on Three-Dimensional Graphene for Supercapacitors. *Nanomaterials* 9:201–210. <https://doi.org/10.3390/nano9020201>
113. Conway BE, Pell WG (2003) Double-layer and pseudocapacitance types of electrochemical capacitors and their applications to the development of hybrid devices. *J Solid State Electrochem* 7:637–644. <https://doi.org/10.1007/s10008-003-0395-7>
114. Wei J-S, Ding H, Zhang P, Song Y-F, Chen J, Wang Y-G, Xiong H-M (2016) Carbon Dots/NiCo<sub>2</sub>O<sub>4</sub> Nanocomposites with Various Morphologies for High Performance Supercapacitors. *Small* 12:5927–5934. <https://doi.org/10.1002/sml.201602164>
115. Liu W, Zhang M, Li M, Li B, Zhang W, Li G, Xiao M, Zhu J, Yu A, Chen Z (2020) Advanced Electrode Materials Comprising of Structure-Engineered Quantum Dots for High-Performance Asymmetric Micro-Supercapacitors. *Adv Energy Mater* 10:1903724. <https://doi.org/10.1002/aenm.201903724>
116. Lee K, Lee H, Shin Y, Yoon Y, Kim D, Lee H (2016) Highly transparent and flexible supercapacitors using graphene-graphene quantum dots chelate. *Nano Energy* 26:746–754
117. Li X, Rui M, Song J, Shen Z, Zeng H (2015) Carbon and graphene quantum dots for optoelectronic and energy devices: a review. *Adv Funct Mater* 25: 4929–4947
118. Lu H, Tournet J, Dastafkan K, Liu Y, Ng YH, Karuturi SK, Zhao C, Yin Z (2021) Noble-Metal-Free Multicomponent Nanointegration for Sustainable Energy Conversion. *Chem Rev* 121:10271–10366. <https://doi.org/10.1021/acs.chemrev.0c01328>
119. Katsounaros I, Cherevko S, Zeradjanin AR, Mayrhofer KJJ (2014) Oxygen Electrochemistry as a Cornerstone for Sustainable Energy Conversion. *Angew Chem Int Ed* 53:102–121. <https://doi.org/10.1002/anie.201306588>
120. Asefa T, Tang C, Ramirez-Hernández M (2021) Nanostructured Carbon Electrocatalysts for Energy Conversions. *Small* n/a:2007136. <https://doi.org/10.1002/sml.202007136>



121. Chu S, Cui Y, Liu N (2017) The path towards sustainable energy. *Nat Mater* 16:16–22. <https://doi.org/10.1038/nmat4834>
122. Hisatomi T, Kubota J, Domen K (2014) Recent advances in semiconductors for photocatalytic and photoelectrochemical water splitting. *Chem Soc Rev* 43:7520–7535. <https://doi.org/10.1039/C3CS60378D>
123. Berardi S, Drouet S, Francàs L, Gimbert-Suriñach C, Guttentag M, Richmond C, Stoll T, Lobet A (2014) Molecular artificial photosynthesis. *Chem Soc Rev* 43:7501–7519. <https://doi.org/10.1039/C3CS60405E>
124. Liu K, Song C, Subramani V (2010) Hydrogen and syngas production and purification technologies. Wiley, Hoboken
125. Fu Y, Dong C-L, Lee W-Y, Chen J, Guo P, Zhao L, Shen S (2016) Nb-Doped Hematite Nanorods for Efficient Solar Water Splitting: Electronic Structure Evolution versus Morphology Alteration. *Chem Nano Mat* 2:704–711. <https://doi.org/10.1002/cnma.201600024>
126. Tong H, Ouyang S, Bi Y, Umezawa N, Oshikiri M, Ye J (2012) Nano-photocatalytic Materials: Possibilities and Challenges. *Adv Mater* 24:229–251. <https://doi.org/10.1002/adma.201102752>
127. Zhang P, Zhang J, Gong J (2014) Tantalum-based semiconductors for solar water splitting. *Chem Soc Rev* 43:4395–4422. <https://doi.org/10.1039/C3CS60438A>
128. Rao VN, Reddy NL, Kumari MM, Cheralathan KK, Ravi P, Sathish M, Neppolian B, Reddy KR, Shetti NP, Prathap P, Aminabhavi TM, Shankar MV (2019) Sustainable hydrogen production for the greener environment by quantum dots-based efficient photocatalysts: A review. *J Environ Manage* 248:109246. <https://doi.org/10.1016/j.jenvman.2019.07.017>
129. Yu H, Zhao Y, Zhou C, Shang L, Peng Y, Cao Y, Wu L-Z, Tung C-H, Zhang T (2014) Carbon quantum dots/TiO<sub>2</sub> composites for efficient photocatalytic hydrogen evolution. *J Mater Chem A* 2:3344–3351. <https://doi.org/10.1039/C3TA14108J>
130. Shi X-F, Xia X-Y, Cui G-W, Deng N, Zhao Y-Q, Zhuo L-H, Tang B (2015) Multiple exciton generation application of PbS quantum dots in ZnO@PbS/graphene oxide for enhanced photocatalytic activity. *Appl Catal B Environ* 163:123–128. <https://doi.org/10.1016/j.apcatb.2014.07.054>
131. Wu H, Li X, Tung C, Wu L (2019) Semiconductor quantum dots: an emerging candidate for CO<sub>2</sub> photoreduction. *Adv Mater* 31:1900709
132. Wu S, Sun J, Li Q, Hood ZD, Yang S, Su T, Peng R, Wu Z, Sun W, Kent PRC, Jiang B, Chisholm MF (2020) Effects of Surface Terminations of 2D Bi<sub>2</sub>WO<sub>6</sub> on Photocatalytic Hydrogen Evolution from Water Splitting. *ACS Appl Mater Interfaces* 12:20067–20074. <https://doi.org/10.1021/acsami.0c01802>
133. Su T, Shao Q, Qin Z, Guo Z, Wu Z (2018) Role of Interfaces in Two-Dimensional Photocatalyst for Water Splitting. *ACS Catal* 8:2253–2276. <https://doi.org/10.1021/acscatal.7b03437>
134. Low J, Cao S, Yu J, Wageh S (2014) Two-dimensional layered composite photocatalysts. *Chem Commun* 50:10768–10777. <https://doi.org/10.1039/C4CC02553A>
135. Zhang M, Wang X (2014) Two dimensional conjugated polymers with enhanced optical absorption and charge separation for photocatalytic hydrogen evolution. *Energy Environ Sci* 7:1902–1906. <https://doi.org/10.1039/C3EE44189J>
136. Heard CJ, Čejka J, Opanasenko M, Nachtigall P, Centi G, Perathoner S (2019) 2D Oxide Nanomaterials to Address the Energy Transition and Catalysis. *Adv Mater* 31:1801712. <https://doi.org/10.1002/adma.201801712>
137. Sugimoto H, Zhou H, Takada M, Fushimi J, Fujii M (2020) Visible-light driven photocatalytic hydrogen generation by water-soluble all-inorganic core-shell silicon quantum dots. *J Mater Chem A* 8:15789–15794. <https://doi.org/10.1039/D0TA01071E>
138. Gao R, Cheng B, Fan J, Yu J, Ho W (2021) ZnxCd1-xS quantum dot with enhanced photocatalytic H<sub>2</sub>-production performance. *Chin J Catal* 42:15–24. [https://doi.org/10.1016/S1872-2067\(20\)63614-2](https://doi.org/10.1016/S1872-2067(20)63614-2)
139. Xiang X, Zhu B, Cheng B, Yu J, Lv H (2020) Enhanced Photocatalytic H<sub>2</sub>-Production Activity of CdS Quantum Dots Using Sn<sup>2+</sup> as Cocatalyst under Visible Light Irradiation. *Small* 16:2001024. <https://doi.org/10.1002/sml.202001024>
140. Li Y, Ding L, Guo Y, Liang Z, Cui H, Tian J (2019) Boosting the Photocatalytic Ability of g-C<sub>3</sub>N<sub>4</sub> for Hydrogen Production by Ti<sub>3</sub>C<sub>2</sub> MXene Quantum Dots. *ACS Appl Mater Interfaces* 11:41440–41447. <https://doi.org/10.1021/acsami.9b14985>
141. Yang F, Liu D, Li Y, Ning S, Cheng L, Ye J (2021) Solid-state synthesis of ultra-small freestanding amorphous MoP quantum dots for highly efficient photocatalytic H<sub>2</sub> production. *Chem Eng J* 406:126838. <https://doi.org/10.1016/j.cej.2020.126838>
142. Wang P, Wang M, Zhang J, Li C, Xu X, Jin Y (2017) Shell Thickness Engineering Significantly Boosts the Photocatalytic H<sub>2</sub> Evolution Efficiency of CdS/CdSe Core/Shell Quantum Dots. *ACS Appl Mater Interfaces* 9:35712–35720. <https://doi.org/10.1021/acsami.7b07211>
143. A. R. SR, Mane RS, Wilson HM, Jha N (2021) Correction: CdSe quantum dot/white graphene hexagonal porous boron nitride sheet (h-PBNs) heterostructure photocatalyst for solar driven H<sub>2</sub> production. *J Mater Chem C* 9:9331. <https://doi.org/10.1039/D1TC90144C>
144. Gao F, Zhao Y, Zhang L, Wang B, Wang Y, Huang X, Wang K, Feng W, Liu P (2018) Well dispersed MoC quantum dots in ultrathin carbon films as efficient co-catalysts for photocatalytic H<sub>2</sub> evolution. *J Mater Chem A* 6:18979–18986. <https://doi.org/10.1039/C8TA06029K>
145. Lei Y, Yang C, Hou J, Wang F, Min S, Ma X, Jin Z, Xu J, Lu G, Huang K-W (2017) Strongly coupled CdS/graphene quantum dots nanohybrids for highly efficient photocatalytic hydrogen evolution: Unraveling the essential roles of graphene quantum dots. *Appl Catal B Environ* 216:59–69. <https://doi.org/10.1016/j.apcatb.2017.05.063>
146. Huang H, Xu B, Tan Z, Jiang Q, Fang S, Li L, Bi J, Wu L (2020) A facile in situ growth of CdS quantum dots on covalent triazine-based frameworks for photocatalytic H<sub>2</sub> production. *J Alloys Compd* 833:155057. <https://doi.org/10.1016/j.jallcom.2020.155057>
147. Yan T, Li N, Jiang Z, Guan W, Qiao Z, Huang B (2018) Self-sacrificing template synthesis of CdS quantum dots/Cd-Hap composite photocatalysts for excellent H<sub>2</sub> production under visible light. *Int J Hydrog Energy* 43:20616–20626. <https://doi.org/10.1016/j.ijhydene.2018.09.093>
148. Xue F, Liu M, Cheng C, Deng J, Shi J (2018) Localized NiS<sub>2</sub> Quantum Dots on g-C<sub>3</sub>N<sub>4</sub> Nanosheets for Efficient Photocatalytic Hydrogen Production from Water. *Chem Cat Chem* 10:5441–5448
149. Kong L, Ji Y, Dang Z, Yan J, Li P, Li Y (2018) S. (Frank) Liu, g-C<sub>3</sub>N<sub>4</sub> Loading Black Phosphorus Quantum Dot for Efficient and Stable Photocatalytic H<sub>2</sub> Generation under Visible Light. *Adv Funct Mater* 28:1800668. <https://doi.org/10.1002/adfm.201800668>
150. Ma B, Xu H, Lin K, Li J, Zhan H, Liu W, Li C (2016) Mo<sub>2</sub>C as Non-Noble Metal Co-Catalyst in Mo<sub>2</sub>C/CdS Composite for Enhanced Photocatalytic H<sub>2</sub> Evolution under Visible Light Irradiation. *Chem Sus Chem* 9:820–824. <https://doi.org/10.1002/cssc.201501652>
151. Liu F, Wang Z, Weng Y, Shi R, Ma W, Chen Y (2021) Black Phosphorus Quantum Dots Modified CdS Nanowires with Efficient Charge Separation for Enhanced Photocatalytic H<sub>2</sub> Evolution. *Chem Cat Chem* 13:1355–1361. <https://doi.org/10.1002/cctc.202001847>
152. Wang J, Chen Y, Zhou W, Tian G, Xiao Y, Fu H, Fu H (2017) Cubic quantum dot/hexagonal microsphere ZnIn<sub>2</sub>S<sub>4</sub> heterophase junctions for exceptional visible-light-driven photocatalytic H<sub>2</sub> evolution. *J Mater Chem A* 5:8451–8460. <https://doi.org/10.1039/C7TA01914A>
153. Jiao Y, Huang Q, Wang J, He Z, Li Z (2019) A novel MoS<sub>2</sub> quantum dots (QDs) decorated Z-scheme g-C<sub>3</sub>N<sub>4</sub> nanosheet/N-doped carbon dots heterostructure photocatalyst for photocatalytic hydrogen evolution. *Appl Catal B Environ* 247:124–132. <https://doi.org/10.1016/j.apcatb.2019.01.073>
154. Shi R, Liu F, Wang Z, Weng Y, Chen Y (2019) Black/red phosphorus quantum dots for photocatalytic water splitting: from a type I heterostructure to a Z-scheme system. *Chem Commun* 55:12531–12534. <https://doi.org/10.1039/C9CC06146K>
155. Sharma V, Kagdada HL, Wang J, Jha PK (2020) Hydrogen adsorption on pristine and platinum decorated graphene quantum dot: A first principle study. *Int J Hydrog Energy* 45:23977–23987. <https://doi.org/10.1016/j.ijhydene.2019.09.021>
156. Xiang C, Li A, Yang S, Lan Z, Xie W, Tang Y, Xu H, Wang Z, Gu H (2019) Enhanced hydrogen storage performance of graphene nanoflakes doped with Cr atoms: a DFT study. *RSC Adv* 9:25690–25696. <https://doi.org/10.1039/C9RA04589A>

## Publisher's Note

Springer Nature remains neutral with regard to jurisdictional claims in published maps and institutional affiliations.